FEDERAL UNIVERSITY OF ITAJUBÁ

MECHANICAL ENGINEERING INSTITUTE

Inverse problems applied to the experimental thermal and hygric analysis of engineering materials

Nícolas Pinheiro Ramos

Itajubá – Minas Gerais – Brazil
2024

FEDERAL UNIVERSITY OF ITAJUBÁ
MECHANICAL ENGINEERING INSTITUTE

Nícolas Pinheiro Ramos

Inverse problems applied to the experimental thermal and hygric analysis of engineering materials

A PhD thesis submitted to the Postgraduate Program in Mechanical Engineering, as a requirement to obtain the Doctorate degree in Mechanical Engineering.

Area of Concentration: Energy, Fluids and Turbomachinery

Advisor: Prof. Dr. Sandro Metrevelle Marcondes de Lima e Silva
Co-advisor: Prof. Dr. Gilmar Guimarães

Itajubá – Minas Gerais – Brazil
2024

FEDERAL UNIVERSITY OF ITAJUBÁ
POSTGRADUATE PROGRAM IN MECHANICAL ENGINEERING

Nícolas Pinheiro Ramos

Inverse problems applied to the experimental thermal and hygric analysis of engineering materials

This PhD thesis was approved by the following advisory committee:

Prof. Dr. Louis Gosselin – Université Laval (ULaval)
Prof. Dr. Roberto Lamberts – Federal University of Santa Catarina (UFSC)
Prof. Dr. Antonio Augusto Araújo Pinto da Silva – Federal University of Itajubá (UNIFEI)
Prof. Dr. Guilherme Ferreira Gomes – Federal University of Itajubá (UNIFEI)
Prof. Dr. Gilmar Guimarães (Co-advisor) – Federal University of Uberlândia (UFU)
Prof. Dr. Sandro Metrevelle Marcondes de Lima e Silva (Advisor) – Federal University of Itajubá (UNIFEI)

Itajubá – Minas Gerais – Brazil
2024

In memory of my beloved grandmothers Betilde and Benedita for their love in every step of my journey.

Acknowledgments

I thank so much my parents, Cecília and Denílson, my sisters, Núbia and Nádia, and my nephew, Benjamin. They have supported me unconditionally and allowed me to get to where I am. I will be always grateful for all the concern, patience, and encouragement dedicated to me.

I would like to especially thank my advisor Sandro, who has been sharing his life experience and scientific knowledge since 2015, and my lab mate Mariana, who has dedicated a lot of time and energy to the development of our studies.

I am also very grateful to my co-advisor Gilmar for the collaboration between LabTC-UNIFEI and LTCME-UFU.

Many thanks to Louis for the opportunity to do a research internship under his supervision at Universté Laval. This is certainly a highlight in my academic journey. I could not fail to acknowledge Leonardo, whose collaboration made my stay in Canada much better.

I would also like to thank all my LabTC colleagues for helping me when I needed it. I must give a special thanks to Carollo, who guided my first steps into the world of experimental inverse heat transfer problems.

I am very grateful to CAPES for my doctoral scholarship.

It is important to highlight the financial support provided by CAPES and UNIFEI's Dean of Research and Postgraduate Studies for my sandwich doctorate.

FAPEMIG is also gratefully acknowledged for its grants and funding.

“Thermodynamically improbable, but here I am.”

Abstract

Ramos, N. P. (2024), *Inverse problems applied to the experimental thermal and hygric analysis of engineering materials*, PhD Thesis, Postgraduate Program in Mechanical Engineering, Mechanical Engineering Institute, Federal University of Itajubá.

Several relevant real-world applications rely on an inverse problem, which involves recovering unknown causes from observing their effects. This differs from the corresponding direct problem, whose solution involves predicting effects from a complete description of their causes. Naturally, inverse problems are more challenging than direct problems because, in general, they are ill-posed, i.e., the solution either does not exist, is not unique or it does not depend continuously on the input data. To soften this problematic aspect, applied inverse modeling requires detailed mathematical-physical modeling and well-designed experiments since the desired parameters are estimated by comparing calculated data with experimental measurements.

In this PhD thesis, inverse approach was applied to experimentally investigate three case studies:

- complementary experiments to simultaneously estimate the parameters describing the temperature-dependent thermal conductivity and specific heat of 304 austenitic stainless steel. Parameter estimation takes advantage of additional information provided by two heat-conducting solids with different geometries. It is an alternative approach to standard thermal characterization techniques, which are often beyond the reach of many laboratories.

- one-year on-site measurements to estimate various hygrothermal properties and thus calibrate the simulation model of a lightweight multilayer wall. A 2D fully coupled heat and moisture transfer model was used to investigate the in-use response of the panel junction region, which is critical in terms of airtightness. The results enable an accurate assessment of building operating conditions by reducing uncertainties in material input data.
- field data to determine the annual heat conduction flux through a wall assembly in an occupied house. Inverse modeling accounted for the physical interactions between outdoor environment and indoor occupancy. The methodology and the findings are useful to support decision-making on energy performance, as there is a lack of long-term field monitoring and information on dynamic heat flux related to prefabricated occupied dwellings.

All the above inverse analyzes were based on evaluating the match between data predicted by numerical simulations in COMSOL Multiphysics and measurements conveying the physical behavior of the component under study. Numerical and experimental data were processed and used for inverse estimation purposes in MATLAB environment. After careful analysis of sensitivity coefficients, different optimization approaches were used to solve the inverse problems. Bayesian statistical inference was applied to determine the estimates and corresponding uncertainties of the thermal properties of 304 stainless steel. The Broyden–Fletcher–Goldfarb–Shanno (BFGS) algorithm, which determines the descent direction by preconditioning the gradient with curvature information, was used in the second case study. The wall heat flux was estimated using the sequential function specification method (SFSM), which expresses temperature as function of heat flux by means of a first-order Taylor series. The results show that inverse modeling is a reliable tool for obtaining valuable information about the hygrothermal mechanisms and parameters involved in applied engineering problems.

Keywords: Inverse analysis, Hygrothermal characterization, Stainless steel, Complementary experiments; Multilayer wall assembly, Occupied prefabricated house, In situ performance.

Resumo

Ramos, N. P. (2024), *Problemas inversos aplicados à análise térmica e higrométrica experimental de materiais de engenharia*, Tese de Doutorado, Programa de Pós-Graduação em Engenharia Mecânica, Instituto de Engenharia Mecânica, Universidade Federal de Itajubá.

Várias aplicações importantes baseiam-se em um problema inverso, que envolve a recuperação de causas desconhecidas a partir da observação de seus efeitos. Já o problema direto correspondente envolve a previsão dos efeitos a partir de uma descrição completa de suas causas. Naturalmente, os problemas inversos são mais complicados do que os problemas diretos porque, em geral, eles são mal-postos, ou seja, a solução não existe, não é única ou não depende continuamente dos dados de entrada. Para amenizar esse aspecto problemático, a modelagem inversa aplicada requer uma modelagem matemática/física detalhada e experimentos bem planejados, já que os parâmetros desejados são estimados pela comparação dos dados calculados com as medições experimentais.

Nesta tese de doutorado, abordagem inversa foi aplicada para investigar experimentalmente três estudos de caso:

- experimentos complementares para estimar simultaneamente os parâmetros que descrevem a condutividade térmica e o calor específico dependentes da temperatura do aço inoxidável austenítico 304. A estimativa de parâmetros aproveita informações adicionais fornecidas por dois corpos condutores de calor com geometrias diferentes. Trata-se de uma abordagem alternativa às técnicas de caracterização térmica padrão, que geralmente estão fora do alcance de muitos laboratórios.

- medições de campo de um ano para estimar várias propriedades higrotérmicas e, assim, calibrar o modelo de simulação de uma parede leve multicamadas. Um modelo 2D de transferência de calor e umidade foi usado para investigar a resposta em uso da região de junção do painel, que é crítica em termos de estanqueidade. Os resultados permitem uma avaliação precisa das condições operacionais da edificação, reduzindo as incertezas nos dados de entrada do material.
- dados de campo para determinar o fluxo anual de condução de calor por meio de uma parede em uma casa ocupada. A modelagem inversa levou em conta as interações físicas entre o ambiente externo e a ocupação interna. Os resultados são úteis para apoiar a tomada de decisões sobre o desempenho energético, pois há uma falta de monitoramento de campo de longo prazo e de informações sobre o fluxo dinâmico de calor relacionado a residências pré-fabricadas ocupadas.

Todas as análises acima basearam-se na avaliação da correspondência entre dados calculados por simulações numéricas no COMSOL Multiphysics e medições que transmitem o comportamento físico do componente em estudo. Os dados numéricos e experimentais foram processados e usados para fins de estimação inversa em ambiente MATLAB. Após uma análise cuidadosa e minuciosa dos coeficientes de sensibilidade, diferentes abordagens de otimização foram usadas para resolver os problemas inversos. Inferência bayesiana foi aplicada para determinar as estimações e as incertezas correspondentes das propriedades térmicas do aço inoxidável 304. O algoritmo Broyden-Fletcher-Goldfarb-Shanno (BFGS), que determina a direção de descida pré-condicionando o gradiente com informações de curvatura, foi usado no segundo estudo de caso. O fluxo de calor através da parede foi estimado usando o método sequencial da função especificada, que expressa a temperatura como função do fluxo de calor por meio de uma série de Taylor de primeira ordem. Os resultados mostram que a análise

inversa é uma ferramenta confiável para obter informações valiosas sobre os mecanismos e parâmetros higrotérmicos envolvidos em problemas de engenharia.

Palavras-chave: Análise inversa, Caracterização higrotérmica, Aço inoxidável, Experimentos complementares; Parede multicamadas, Casa pré-fabricada ocupada, Desempenho in situ.

List of figures

List of tables

Contents

1. Introduction

1.1 Fundamentals of inverse problems

The French mathematician Jacques-Salomon Hadamard studied the nature of mathematical models to accurately represent physical phenomena and the defined the concept of well-posed and ill-posed problems[1].

These are the conditions for a problem to be considered well-posed according to Hadamard:

- There must exist a solution.
- The solution must be unique.
- The solution must depend continuously on the input data or the initial and boundary conditions.

A physical problem that does not satisfy all the criteria mentioned above is considered an ill-posed problem. All physical interactions between a body with its surroundings can be related to cause-and-effect problems [2]. For instance, in a heat transfer model, the causes are the initial and boundary conditions, thermal properties, heat generation sources, and geometrical characteristics. The effect, in turn, is the time evolution of the temperature distribution throughout the studied body. For a direct problem, the causes are known, and the effects are unknown and need to be determined. Most engineering studies are conducted in a direct (forward) manner, usually focusing on determining the effects. Direct problems are well-posed problems and remain stable for small changes in input data. On the other hand, an inverse problem is a problem where the effects are measured and then used to determine one or more causes. In other words, inverse problems occur in a backward manner, i.e., they are governed in the opposite direction to nature. Since it is impossible to reverse time, the causality of nature prevents inverse problem solutions from being experimentally reproduced. This would imply a violation of the cause-and-effect relationship [3]. Inverse problems are naturally ill-posed. Most often, Hadamard's third criterion is not satisfied for this type of problem, and the second criterion is not satisfied sometimes either.

1.2 Parameter estimation versus function estimation

Inverse problems can be categorized into two classes [4]: parameter estimation and function estimation. In parameter estimation, a small number of parameters are to be estimated. By contrast, the number of unknown elements is generally high for function estimation, since a profile is estimated rather than strict values. Parameter estimation is usually concerned with the characterization of physical properties, which are not exposed to human influence or adjustments. Results of parameter estimations are usually given with confidence intervals and are only valid in the range covered by the experiments performed. This is not the case with a function estimation, where the estimates are inherent to the problem at hand. Unlike function estimations, parameter estimations deal with sought-after quantities that behave differently according to measurement variations. This implies that much more caution is required when designing and conducting experiments for parameter estimation purposes [4]. It is therefore crucial to perform a careful sensitivity analysis to increase estimation accuracy [5].

Although solving inverse problems is very useful, their ill-posedness makes the governing sensitivity matrices ill-conditioned and sometimes rank deficient. Ill-posedness means that the existence of a unique solution cannot be guaranteed for small changes in the measurements, and there may be a long, narrow valley of solutions. Also on this matter, inverse analyzes of practical interest are constructed based on physical measurements, and measurements always contain errors. The same measurements taken under the same conditions but at different times are very likely to be different. Thus, real-world inverse problems are naturally noisy, and the results may not correspond fairly to the system being studied due to inaccuracies in data collection. To soften the difficulties related to this ill-posed character, a good awareness of model imperfections and measurement uncertainties is required [6] .

1.3 Inverse problem solution

Methods for solving inverse problems have been extensively researched and discussed [4], [7]. However, none are absolute and universally applicable [8] . This is because the correct choice of the optimization technique mainly depends on the kind of the problem at hand, with an approach being expected to be efficient for a given problem and work poorly for another [9]. In general, optimization techniques for computing inverse solutions can be roughly categorized into gradient-based and stochastic (probabilistic) methods.

The gradient-based approaches are exact mathematical methods and are more frequently used. These classical methods have fast convergence speed, high accuracy, and effectiveness as advantages. Nevertheless, as they use information about the slope of the objective function to define the search direction, calculating surface gradients and sensitivity coefficients is mandatory. Computing sensitivity derivatives is laborious when multidimensional, nonlinear, multimodal, discontinuous, and transient cases are considered. Gradient methods are not free from the “local minima trap” problem, which means to search for a local optimum solution instead of a global optimum one [10]. They can exploit a limited search region around a given starting value, but they tend to fail when the starting value is far from the global solution [11] . Thus, these methods can be very inefficient to find good solutions when they are employed to minimize functions that have flat valleys, as is the case for the one at hand. The valley is easily found, but the converge to the global minimum lying inside the valley is difficult or even impossible. Along the valley, the function is very insensitive to changes in the desired parameters. This means that the bottom surface of the objective function is not strongly convex in the optima neighborhoods. Gradient-based methods are stable only if the Hessian matrix is positive definite, and they can even diverge if the initial guess is too far from the optimum [12].

The term stochastic may refer to random processes that can represent a system which evolution over time is described by combing available data (current and past knowledge) and predicted successive changes (future knowledge) [9]. Stochastic methods are approximation methods that do not depend on gradient fields for optimization. They generate and analyze random variables to find sufficiently adequate solutions to optimization problems. Since they search in a random way, derivative-free optimization methods have no perfect repeatability and can be more computationally efficient compared with gradient-based methods. However, they can be time-consuming when handling very simple problems, given the computational costs for iteratively achieving convergence [13], [14]. Additionally, stochastic methods are less susceptible to the “local minima trap”, obtaining the best solution that can be possibly found after a given number of iterations. Such techniques have been successfully used to solve inverse problems [15], [16], [17] and are very relevant in assessing engineering problems with complicated relationships between design variables [13]. Probabilistic methods can be helpful when dealing with ill-posed problems since they provide proper solutions from a population of good individuals (optimal points) or from a probability density (mean and standard deviation values).

1.4 Application of inverse problems

Inverse problems are a robust and effective tool to indirectly estimate quantities appearing in the mathematical formulation of physical phenomena [4]. Inverse analyzes are found in multi-scale physical processes, and applications range from the identification of constant parameters to the tracking spatial- and time-dependent functions [7]. Inverse methodologies are also constantly involved in everyday activities, such as medical imaging and dynamic aircraft position prediction [7]. A typical example is related to inferring information about the interior of a sample subjected to a scanning process from measured data on its surface [18].

The background needed to properly apply inverse approach to evaluate real engineering problems consists of the following functional milestones [18]:

- Mathematical modeling (inverse problem formulation, including governing equations, geometry, sources, coefficients, and initial and boundary conditions).
- Mathematical analysis (existence, uniqueness, stability).
- Numerical modeling (physics-based simulations or computational codes).
- Design of experiments (optimal placement of sensors, duration of measurements, configuration of experimental parameters).
- Experimental analysis (performing experiments to measure data that will serve as information for inverse problem solution).
- Computational analysis (implementation of programing codes to integrate the previous analyzes and process the raw data and results).

Therefore, different knowledge and tools are required to thoroughly accomplish the above tasks, which makes inverse approach highly interdisciplinary.

1.5 Research objectives

Thermal and hygric characterization of materials and structures are critical to obtain knowledge of their operational behavior. However, direct measurement or access to standard thermal characterization methods are often complicated due to experimental and financial issues. In this context, this research work seeks to employ inverse methodologies to the thermal and hygric analysis of different engineering materials. Three case studies are experimentally investigated in this PhD thesis:

In chapter 2, two complementary transient experiments are carried put to provide robust information to simultaneously estimate the parameters describing the temperature-dependent thermal conductivity and specific heat of 304 austenitic stainless steel.

In chapter 3, one-year on-site measurements are used to estimate various hygrothermal properties and thus calibrate the simulation model of a lightweight multilayer wall.

In chapter 4, the annual dynamic heat conduction flux through a wall assembly is estimated from field data measured in an occupied house.

Chapter 5 presents a general conclusion to this research work, providing an overview on the main aspects addressed.

Finally, an outlook on the activities carried out during the doctorate is presented in the Appendix.

2. Case Study 1: Complementary Experiments to Estimate the Thermal Properties of 304 Austenitic Stainless Steel

2.1 Austenitic stainless steel

The capacity of handling metallic materials has changed human history since Metal Ages. With the industrial revolution, the use of metals and their alloys in human activities increased rapidly owing to their distinct characteristics [19]. In today's highly energy-dependent society, technological progress and innovation depend on using metals, which are widely employed in numerous engineering applications. Metals offer quality, efficiency, and safety for human activities. They are necessary inputs used in providing essential services and products worldwide, like in the transportation, construction, telecommunications, and energy production and distribution sectors [19].

Stainless steels (SSs) are a very relevant group of metal alloys, since they are used in a large variety of applications, varying from everyday use in kitchen utensils and furnishings, to very advanced uses in the oil & gas, chemical, and aerospace industries. They are valued for their corrosion resistance, durability, strength, and aesthetic appeal. Stainless steels can be basically categorized into three groups according to their microstructure: ferritic, austenitic, and martensitic. These different metallurgical structures are obtained by modifying steel chemistry. To achieve specific properties, SSs contain substantial amounts of alloying elements, mainly chromium and nickel, but also molybdenum, silicon, carbon, nitrogen, and manganese [20] .

There are over 150 grades of stainless steel, each with its particular properties. 300 series is a grade of austenitic stainless steel (ASS) and is the most used grade worldwide. 300-series

ASSs are used in mandatory heat-resistant structural applications given their properties regarding corrosion resistance, mechanical strength, metallurgical stability, fracture toughness, and ductility at high temperatures [20]. There are two important types of 300 austenitic stainless steels: 304 and 316. 304 ASS is used in about 60% of all applications. As they are austenitic, 304 ASS and 316 ASS are non-magnetic and have a low carbon content. This makes them highly weldable and formable. These two heat-resisting alloys are comparable in terms of mechanical properties and differ moderately in chemical composition. Generally, 304 ASS has more chromium and less nickel compared with 316 ASS. 316 ASS also incorporates approximately 2% molybdenum, which increases strength and chemical corrosion resistance [21]. Concerning their thermal behavior, it is known that chemical composition most considerably controls the thermal conductivity (k) and specific heat (c_p) of alloy steels [22]. Alloying elements also impact both thermal properties, which usually decrease with increasing the alloying degree [23]. Thus, 304 ASS has moderately higher c_p and k in comparison with 316 ASS [24] .

2.2 Thermal characterization of metallic materials

Materials characterization is essential for evaluating the thermal behavior of a particular domain, since the robustness of thermal analyzes depends on how reliable the properties of the system being studied are. Reliable thermal property data lead to better results when designing, optimizing, and implementing heat transfer processes [12]. Additionally, temperature dependence is a key condition for metals because they are widely employed in temperature-varying applications. Considering thermal properties as constants can mislead to unrealistic numerical simulations when predicting materials' response to changes in the working temperature [25]. Thus, methods for determining accurate temperature-dependent thermal properties of metallic materials are fundamental to thermal sciences.

Thermal properties of conducting materials, like metals, cannot generally be obtained via direct measurements. As a result, experiments can be designed and performed for measuring temperature and/or heat flux data which are further used in combination with mathematical expressions to determine the desired thermal parameter(s) [12]. Standardly, there are three different approaches for obtaining the thermal properties of a material. The first one consists of steady-state measurements of heat flux and temperature gradients, as in the guarded hot plate method [26]. Despite the high accuracy, this group of techniques is very time-consuming and can hardly ever be applied to high conducting materials. Also, they require specialized equipment and can furnish only thermal conductivity. The calorimetric approach, on the other hand, is very well suitable when the target is to obtain c_p. Differential scanning calorimetry (DSC), for example, has been extensively applied for this purpose. Nevertheless, these methods do not furnish thermal conductivity and manage to provide thermal properties only for high-temperature levels. Moreover, they also require specific and expensive equipment, and difficulties arise when dealing with inhomogeneous materials, due to the mandatory small sample size [27]. Lastly, the third approach introduces transient techniques, such as the transient hot wire method [28] and the laser flash method [29]. For both techniques, thermal conductivity and thermal diffusivity can be obtained (not simultaneously) within a much smaller period than that needed in steady-state experiments. Anyhow, the experimental assemblies also demand considerable financial and time resources for obtaining each thermal property. All these classical techniques have already been improved, yet, none of them is unrestricted, which means that methods for obtaining thermal properties are usually defined for specific materials and temperature ranges [12], [26].

Apart from the classical techniques, several novel methods for thermal characterization have been developed for engineering material applications [30]. These techniques should seek a trade-off between reliable outcomes and reasonable computational and experimental costs. Transient experimental methods for estimating the thermal properties of high-conducting materials are scarce. This is because it is difficult and expensive to design and carry out transient experiments for thermally characterizing metals, due to contact resistance effects and thermal sensitivity deficiencies when dealing with these materials [31]. Additionally, considerable efforts and expertise are needed to obtain well-planned and well-conducted experiments for thermal characterization. For these reasons, thermal characterization approaches for analyzing metallic materials are somewhat limited; there are not many approaches that can be used in these materials [32], [33], [34]. Some of these novel methods disregard temperature dependence [31], [35]. Several techniques cannot perform simultaneous estimations, assessing only one property, or requiring more than one process to achieve others [36]. Also, they generally do not consider data from the entire temperature domain. Naturally, techniques that seek to simultaneously estimate temperature-dependent thermal properties have also been studied and presented. Most evaluate temperature dependence using data regressions within small temperature ranges and do not consider data corresponding to the entire temperature domain [37], [38]. These approaches require several experiments or numerical simulations where the sample is subjected to different initial conditions. Finally, many approaches have not been experimentally validated, and have focused on only numerical or analytical analyzes [38], [39], [40].

Here, a linear variation of $k(T)$ and $c_p(T)$ in temperature is assumed and the constant and slope defining these functions are estimated. Previous studies, as per Mohebbi et al. [39], [41], [42], have shown that it is feasible to determine parameters for a linear form describing the temperature dependence of the thermal properties. However, it turns out that these papers cover theoretical background on inverse heat conduction, since they perform analyzes from numerically simulated temperature data. In addition to not presenting experimental validation, their techniques were applied to a generic solid medium [39] or to insulation materials [41], [42] which does not lead to great difficulties concerning rank deficiency and valley bottom landscape.

Thermal conductivity and specific heat of the metallic material used are needed to obtain knowledge of the thermal behavior of metal parts present in engineering structures. However, access to standard thermal characterization methods is often complicated due to financial issues. In this context, this study seeks to present a simple experimental approach for simultaneously identifying the linearly temperature-dependent k and c_p of 304 austenitic stainless steel. Parameter estimation takes advantage of a relevant sensitivity increase, provided by two complementary transient experiments. Bayesian inference is used to analyze the accordance between experimentally measured and numerically calculated temperatures. Inverse thermal analysis is based on two heat-conducting solids with different geometries. In estimation problems, one seeks to obtain as much data as possible using as few sensors as possible. So, single thermocouple data are collected for each thermal model. The proposed technique provides a cost-effective and robust thermal property estimation from tests conducted at room temperature. Single-step estimation incorporates data from the whole temperature domain and infers a set of four parameters for linear functions representing the temperature dependence of k and c_p. This means that the linear relationship between thermal property and temperature is directly determined, with no need for fitting a regression line. Since the inverse methodology provides k and c_p at once, two or more different procedures are not required for obtaining both thermal properties, unlike most standard tests for measuring the thermal properties of metallic materials. The contact resistance effect at the heater-metal interface is evaluated at microscopic level and set as a reducing factor in the heat flux load supplied to the samples.

2.3 Complementary data

Complementary data are important because they can furnish additional information that can help to support or refute a hypothesis. Complementary data can also be used to generate new hypotheses or to help understand complex phenomena [43]. It is important to ensure that the collected data are as high quality as possible and that they come from a variety of sources [43]. The supplementary information provided by complementary experiments can improve the robustness of estimation procedures [43].

Parameter estimation is the process of using observations to estimate the values of parameters for a model. In many scientific disciplines, parameter estimation is an important task that allows researchers to make predictions and understand the behavior of a system [4]. The quality of the estimates depends on both the quality of the data and the chosen model. In parameter estimations, we need as much data as possible to give a solid basis to the optimization algorithm to find a solution that can reliably represent the studied physical phenomenon, in an acceptable error sense. Complementary data can be used to improve parameter estimation by providing more robust information that can help to constrain or identify the values of parameters. This is especially relevant when there are few observations or when they are noisy, as complementary data can help to reduce uncertainty and improve reliability. Additional information from complementary thermal models can enable simultaneous estimations with multiple objectives, since they decrease or even avoid rank deficiency [44]. Rank deficiency in this context basically means the lack of sufficient information in the available data to estimate the desired parameters. As the quantity of parameters to be found raises, data from complementary events enhances the robustness of inverse analyzes.

There are several reasons why complementary experiments contribute to obtaining better parameter estimation. First, different experiments may be sensitive to different aspects of the system under study. This can enable for more complete coverage of the parameter space and reduce the uncertainty in the estimates. Second, different experiments may have different levels of precision. Complementary experiments can help to average out errors and improve the overall accuracy of the estimates. Finally, some types of experiments may be more expensive or difficult to carry out than others. By using a combination of experiment types, researchers can minimize costs while still obtaining reliable results [43].

Complementary data have been used in inverse problems of different fields of study. For instance, Boyd and Little [45] analyzed the application of complementary data to limited-angle computed tomography. Weichman et al. [46] used complementary information in an inverse problem to infer subsurface water distribution from Nuclear Magnetic Resonance (NMR) voltage measurements. Led and Gesmar [47] showed the importance of complementary experiments to determine chemical exchange rates using magnetization-transfer NMR technique. Cao et al. [48] used complementary data to boost the image quality of low-resolution sensors using super-resolution technique.

Complementary experiments have not been explored much to estimate thermal properties and have never been applied to metallic materials. McMasters et al. [44] studied the increase in sensitivity when using complementary one-dimensional heat conduction experiments to estimate constant thermal properties. Mehta et al. [49] inferred the temperature-dependent thermal conductivity and volumetric heat capacity of sweet potato puree using sequential parameter estimation. Benyathiar et al. [50] studied the optimal design of complementary experiments to simultaneously estimate the temperature-dependent thermal properties of sweet potato puree.

The combination of complementary data can reduce the correlation between desired parameters, improving the confidence region of estimates [44]. Further, the use of complementary experiments can improve the sensitivity coefficients of the parameters of interest [50]. The target is to maximize the information that can be obtained from such experiments [44]. This is particularly significant for k, which usually has low sensitivity coefficients for transient models. Low sensitivity coefficients lead to significant difficulties when using mathematical programming techniques, since sensitivity and information matrices must be calculated in these methods. If there are insufficient suitable initial guesses, and large and uncorrelated sensitivity coefficients, the inverse solution diverges and fails when using classical gradient-based methods. This greatly restricts the search space and is not desirable when investigating materials that have not yet been thermally characterized.

2.4 Thermal problem modeling

2.4.1 One-dimensional thermal model

The first thermal model, shown in Figure 1a, considers transient nonlinear one-dimensional heat conduction over an isotropic plate, where phase change, convection, radiation, and heat generation are neglected. Thermal properties are considered to vary linearly with temperature, as per: $k = A + B \times T$, and $c_p = C + D \times T$; with parameters A, B, C and D being simultaneously estimated. The metal plate is uniformly heated on the top surface using a constant heat flux load. Thermal insulation condition is maintained on the bottom surface, where temperature information is measured from a single sensor. Thus, the thermal problem is governed by the heat diffusion equation expressed as follows:

$$\frac{\partial}{\partial x}\left(k\frac{\partial T}{\partial x}\right) = \rho c_p \frac{\partial T}{\partial t}, \qquad 0 \le x \le L,\ t > 0 \tag{1}$$

where x is the direction of heat transfer; ρ is the constant density; t is the time; and T is the temperature, which is a function of x and t, i.e., $T = T(x, t)$.

Equation (2) and Equations (3)-(4) describe, respectively, the initial and boundary conditions to which the 1D model is subjected.

$$T(x, 0) = T_{in}, \qquad 0 \le x \le L,\ t = 0 \tag{2}$$

$$-k\left.\frac{\partial T}{\partial x}\right|_{x=0} = \frac{T_h - T_p}{R_c}, \qquad \text{at } x = 0,\ t > 0 \tag{3}$$

$$\left.\frac{\partial T}{\partial x}\right|_{x=L} = 0, \qquad \text{at } x = L,\ t > 0 \tag{4}$$

where T_{in} is the initial temperature; T_h and T_p are the temperatures of the heater and plate at the contact point, respectively; L is the plate thickness; and R_c is the contact resistance, i.e., the reciprocal of the contact conductance h_c. R_c causes a decrease in the amount of heat conducted to the metallic sample, i.e., it represents a reducing factor in the heat flux load (q), supplied by the resistive heater.

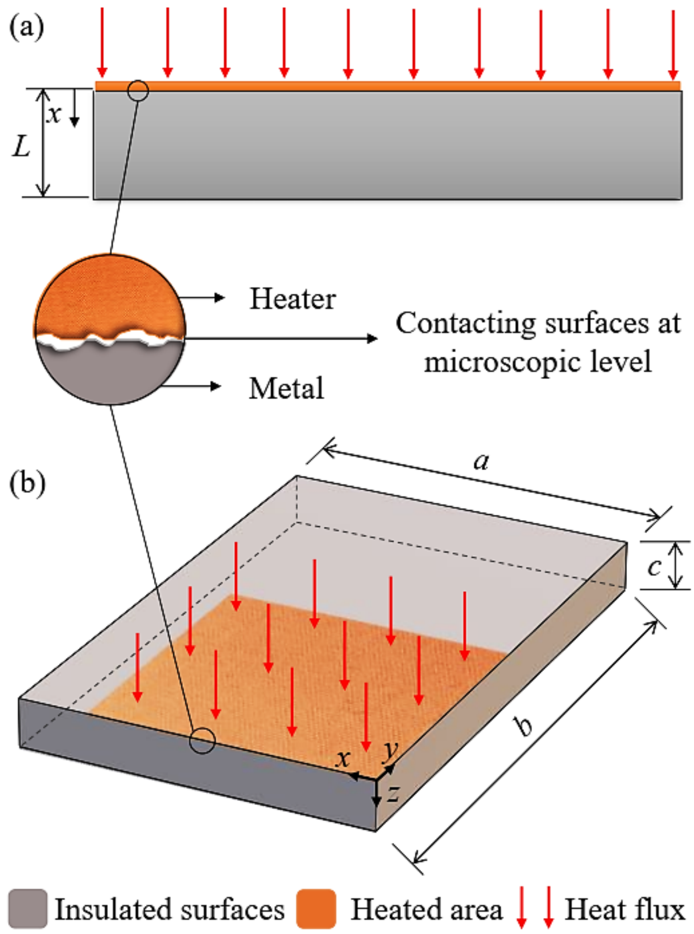

Figure 1. Schematic of the complementary heat conduction models: a) 1D thermal model; b) 3D thermal model.

The contact conductance existing at the heater-plate interface is due to two factors: i) the presence of air, causing interstitial conductance ($h_{interstitial}$), which is evaluated using the parallel-plate gap gas correlation and basically corresponds to the convection coefficient of the interstitial fluid; ii) and the contact spots, responsible for the constriction conductance ($h_{constriction}$). Radiation effects can be neglected because the experimental setup is kept below 400 °C [51]. Convection effects can also be disregarded since the interface gap thickness is too small to allow convection current [52].

The Cooper-Mikic-Yovanovich (CMY) correlation is used to calculate $h_{constriction}$. CMY correlation associates the constriction conductance with microscopical characteristics and compression load at the contacting interface, as follows [53]:

$$h_{constriction} = 1.25 k_{contact} \frac{s_{asp}}{r_{asp}} \left(\frac{p}{H_c}\right)^{0.95} \tag{5}$$

where $k_{contact}$ is the thermal conductivity harmonic mean of the two materials in contact; H_c is the hardness of the softer material; p is the contact pressure; and s_{asp} and r_{asp} are, respectively, the average slope and roughness of the contact asperities.

The interstitial conductance is computed by the correlation shown below:

$$h_{interstitial} = \frac{k_{if}}{\Upsilon + M_g} \tag{6}$$

where k_{if} is the thermal conductivity of the interstitial fluid; Υ is the mean separation thickness between the surfaces; and M_g is the gas parameter.

The contact resistance methodology used here is more completely presented in Ramos et al. [31], where the joint conductance at two contacting surfaces is assessed at microscopic level.

2.4.2 Three-dimensional thermal model

Consider a three-dimensional transient nonlinear heat conducting body. In the 3D thermal model (Figure 1b), the top surface is partially heated with a constant heat flux intensity. The isotropic metal plate is thermally insulated on all other surfaces. The thermal properties depend only on temperature, following the same linear relationship as the 1D formulation. Again, convection, heat generation, phase change, and radiation effects are neglected. Thus, this 3D direct problem can be described mathematically by Equation (7). The initial condition is given in Equation (8) and the boundary conditions in Equations (9)-(11). Two different thermal boundary conditions are applied to the upper surface (S). The boundary condition at the heated region (S_1) considers the thermal contact between the heater and the metallic plate. The rest of the upper surface (S_2) has a thermal insulation boundary condition.

$$\frac{\partial}{\partial x}\left(k\frac{\partial T}{\partial x}\right)+\frac{\partial}{\partial y}\left(k\frac{\partial T}{\partial y}\right)+\frac{\partial}{\partial z}\left(k\frac{\partial T}{\partial z}\right) = \rho c_p \frac{\partial T}{\partial t}, \quad 0 \le x \le a,\ 0 \le y \le b,\ 0 \le z \le c,\ t > 0 \tag{7}$$

$$T = T_{in}, \quad 0 \le x \le a,\ 0 \le y \le b,\ 0 \le z \le c,\ t = 0 \tag{8}$$

$$-k\left.\frac{\partial T}{\partial z}\right|_{z=0} = \frac{T_h - T_m}{R_c}, \quad \text{at } S_1,\ t > 0 \tag{9}$$

$$\left.\frac{\partial T}{\partial z}\right|_{z=0} = 0, \quad \text{at } S_2,\ t > 0 \tag{10}$$

$$\left.\frac{\partial T}{\partial x}\right|_{x=0} = \left.\frac{\partial T}{\partial x}\right|_{x=a} = \left.\frac{\partial T}{\partial y}\right|_{y=0} = \left.\frac{\partial T}{\partial y}\right|_{y=b} = \left.\frac{\partial T}{\partial z}\right|_{z=c} = 0, \qquad t > 0 \tag{11}$$

where T depends on Cartesian coordinates (x, y, z) and time t, i.e., $T = T(x, y, z, t)$; a, b and c are the sample linear dimensions; S_1 is the region at the top surface where the heat flux is imposed, and is limited to ($0 \leq x \leq l_H$, $0 \leq y \leq l_H$, $z = 0$); l_H is the square section heater length, which is the boundary of the heated region S_1; and S_2 is the other portion of the top surface, which is subjected to thermal insulation. Thermal insulation is applied to all other domain boundary surfaces.

2.5 Bayesian inference for inverse solution

For the two heat conduction problems described above, one can formulate direct problems in which geometry, thermal properties, and initial and boundary conditions are known. These direct problems are solved to determine the transient temperature distribution in the metallic samples. On the other hand, it is also possible to deal with an inverse problem for which the thermal conductivity and specific heat are taken as unknown. The solution to this inverse problem, which seeks to estimate the quantities of interest (k and c_p), is feasible using transient temperature measurements. In the inverse thermal problem assessment, parameters for the thermal properties as linear functions of temperature are unknown quantities. Complementary transient temperature histories are measured at discrete time steps and then used to retrieve the vector containing the desired parameters $\mathbf{P} = [A, B, C, D]$. Thus. the inverse problem under consideration is defined and evaluated as an optimization problem, where the temperature distributions of both thermal models are numerically calculated, and then compared to experimentally measured temperatures. The simultaneous inverse estimation of the linearly temperature-dependent thermal conductivity and specific heat of 304 ASS is performed considering data from the whole temperature domain.

The Bayesian inference is a stochastic manner of optimization. The Bayesian approach to statistics considers the inverse problem solution as a statistical inference based on analyzing the posterior probability distribution [54], [55]. The objective is to explore the posterior distribution related to the probability of a range of values for the unknown parameters, given temperature measurements. This condition makes statistical approaches considerably different from traditional deterministic techniques. Deterministic methods obtain single estimates of the unknown parameters whereas statistical methods do not generate only single estimates. Rather, the framework of Bayesian statistics produces a distribution that is employed to determine estimates that have different probabilities. Bayesian inference can assess not only knowledge regarding the uncertainties associated with the estimates, but also intrinsic regularization is provided to the inverse problem so that it can be turned into a well-posed problem [56]. As inserting subjective prior information is a fundamental principle of the Bayes' theorem, this statistical-based method is affected by initial guesses [56].

The Bayesian approach employs measurements as a foundation for establishing a "Gaussian tent" over these measured data, provided that the results can be well represented by a Gaussian distribution. This probabilistic regularization smooths the ill-posedness of the inverse problem and attempts to statistically account for unavoidable variations in the measurements [56]. In Bayesian estimation, the prime target is to infer the probability distribution of unknown quantities from available data (current and previous information), also named the posterior probability density function (PPDF). The Bayesian inference is based on the Bayes' theorem, which is stated as follows according to Kaipio and Fox [57]:

$$\pi_{posterior}(Z) = \pi(Z|Y) = \frac{\pi(Y|Z)\pi(Z)}{\pi(Y)} \tag{12}$$

where Z denotes the hypothesis (missing parameters, vector or scalar); Y represents the observations/ measurements (vector), i.e., the observed data related to the hypothesis; $\pi(Z|Y)$ is the PPDF, i.e., the conditional probability of Z given the observations Y; $\pi(Y|Z)$ is the likelihood function, which is the conditional probability density function of the observations Y considering missing the unknown parameters Z; $\pi(Z)$ is the prior density function (PDF), i.e., a statistical representation for the knowledge about the unknown parameters prior to the observations; $\pi(Y)$ is the marginal likelihood, which assesses the model fit and acts as a normalizing constant of Bayes' theorem. Therefore, after having observed Y, Bayes' formula is employed to obtain the distribution of Z conditional on Y, i.e., the posterior probability of the hypothesis considering some observations is achieved by multiplying its likelihood and prior probability.

An outlook on Bayesian inference on estimating thermal parameters is addressed here. Generally, the thermal properties of conducting materials cannot be directly measured. As a result, one can design experiments to obtain temperature measurements to solve an inverse problem to estimate the related and unknown quantities. In this sense, the thermal properties can be assumed as random variables and Bayesian inference can be employed to reconstruct the probability density functions of **P** given the transient temperature measurements and thermal model.

Techniques based on Bayesian inference have proved their applicability to this kind of inverse problem since the temperature response is known to be a sufficient statistic of k and c_p [56]. Bayes' theorem is the mathematical method used to integrate new available data with previously obtained information. Markov chain Monte Carlo (MCMC) sampling was used to solve the inverse problem and then to evaluate the posterior distribution. MCMC sampling methods are feasible approaches for computing estimates in cases where the quantity of unknown parameters is not very large [55]. These methods usually lead to computationally demanding solutions, which is a practical disadvantage. The inverse problem is solved by sampling candidate values from the PDF and evaluating them through the thermal model that generates results that are compared with the measured data through the likelihood function. All available knowledge is used to reduce the uncertainty present in a primary assumption related to inferential statistics. As new knowledge is achieved, there is a combination of previous and current information to devise the base for statistical processes. A candidate value that is consistent with the data receives a higher probability than a candidate value that is not. The evaluation of the thermal model and the update process from PDF to PPDF occurs simultaneously.

Let **Y** denote the vector containing the experimentally measured temperatures, as follows:

$$\mathbf{Y}^{\mathrm{T}} = [\mathbf{Y}_1, \mathbf{Y}_2, \dots, \mathbf{Y}_N] \tag{13a}$$

with

$$\mathbf{Y}_i = \left[Y_{1\mathrm{D}_i}, Y_{3\mathrm{D}_i}\right] \qquad \text{for } i = 1, \dots, N \tag{13b}$$

where N are the number of measurements; and $Y_{1\mathrm{D}}$ and $Y_{3\mathrm{D}}$ are the components of $\mathbf{Y}_{1\mathrm{D}}$ and $\mathbf{Y}_{3\mathrm{D}}$, the vectors of temperature measurements from the 1D and 3D experiments, respectively.

The vector **P** is introduced into Bayes' theorem as the hypothesis *Z*, associating the inverse problem of interest here with the Bayesian inference. The Bayesian formulation for the simultaneous estimation is described in detail next:

$$\pi_{posterior}(\mathbf{P}) = \pi(\mathbf{P}|\mathbf{Y}) = \frac{\pi(\mathbf{Y}|\mathbf{P})\pi(\mathbf{P})}{\pi(\mathbf{Y})} \tag{14}$$

The calculation of the marginal probability density of the measurements $\pi(\mathbf{Y})$ can usually be ignored for a functional application of Bayes' formula since $\pi(\mathbf{P}|\mathbf{Y})$ must be a proper probability distribution. The PPDF can be thus rewritten as the product of $\pi(\mathbf{Y}|\mathbf{P})$ and $\pi(\mathbf{P})$, as follows:

$$\pi_{posterior}(\mathbf{P}) = \pi(\mathbf{P}|\mathbf{Y}) \propto \pi(\mathbf{Y}|\mathbf{P})\pi(\mathbf{P}) \tag{15}$$

The posterior distribution was estimated by the Metropolis-Hastings algorithm (MH-MCMC), the most popular Markov chain algorithm [55]. The implementation of the Metropolis-Hastings algorithm is performed by initially choosing a jumping distribution $p(\mathbf{P}^*, \mathbf{P}^{n-1})$, which is a probability density employed to obtain a new state $\mathbf{P}^*$ given the current state $\mathbf{P}^{n-1}$ of the Markov chain. After selecting this proposal distribution, the following steps must be repeated until achieving the total number of states *G*:

1. Take the state *n* of the Markov chain and draw a sample $\mathbf{P}^*$ from a jumping distribution $p(\mathbf{P}^*, \mathbf{P}^{n-1})$;
2. Solve the direct problem using $\mathbf{P}^*$;

3. Compute the posterior $\pi(\mathbf{P}^*|\mathbf{Y})$;

4. Compute the acceptance function:

$$\alpha = min\left[1, \frac{\pi(\mathbf{P}^*|\mathbf{Y})p(\mathbf{P}^{n-1}, \mathbf{P}^*)}{\pi(\mathbf{P}^{n-1}|\mathbf{Y})p(\mathbf{P}^*, \mathbf{P}^{n-1})}\right]; \tag{16}$$

5. Generate a random value U which is uniformly distributed on (0,1);

6. If $U \leq \alpha$, define $\mathbf{P}^n = \mathbf{P}^*$; otherwise, define $\mathbf{P}^n = \mathbf{P}^{n-1}$;

7. Set $n = n + 1$ and return to step 1.

In such a way, the sequence $\{\mathbf{P}^1, \mathbf{P}^2, \mathbf{P}^G\}$ representing the posterior distribution is generated. The inference on this distribution is determined from analyzing the samples $\mathbf{P}^n$. It is important to notice that $\mathbf{P}^n$ values must only be considered after the chain has reached convergence to equilibrium. More theoretical details on MH-MCMC can be found in Kaipio and Fox [57].

Normal distributions are suitable to statistically characterize thermocouple measurements because of the central limit theorem. Measurement errors are usually the result of many other errors, and the combination of these errors leads to normality. Therefore, the measurement errors are taken as Gaussian random variables, additive and independent of the sought parameters $\mathbf{P}$. Thus, the likelihood function can be given as follow according to Wang and Zabaras [56]:

$$\pi(\mathbf{Y}|\mathbf{P}) = \frac{1}{(2\pi)^{N/2}|\mathbf{W}|^{1/2}} exp\left\{-\frac{1}{2}[\mathbf{Y} - \mathbf{T}(\mathbf{P})]^{\mathrm{T}}\mathbf{W}^{-1}[\mathbf{Y} - \mathbf{T}(\mathbf{P})]\right\} \tag{17}$$

where **T**(**P**) is the numerical solution of the direct problems with a given **P** at specific sensing locations. **T** is given in function of the components of $\mathbf{T}_{1D}$ and $\mathbf{T}_{3D}$, the vectors containing the numerical temperatures from the direct 1D and 3D thermal problems, respectively.

$$\mathbf{T}^{\mathrm{T}} = [\mathbf{T}_1, \mathbf{T}_2, \dots, \mathbf{T}_N] \tag{18a}$$

with

$$\mathbf{T}_i = \left[T_{1\mathrm{D}_i}, T_{3\mathrm{D}_i}\right] \qquad \text{for } i = 1, \dots, N \tag{18b}$$

W is the covariance matrix of the measurement errors, which, for uncorrelated measurements, is given in the following form:

$$\mathbf{W} = \begin{bmatrix} \sigma_{Y_1}^2 & \cdots & 0 \\ \vdots & \ddots & \vdots \\ 0 & \cdots & \sigma_{Y_N}^2 \end{bmatrix} \tag{19}$$

The uncertainty σ_Y is due to the experimental temperature errors, which are assumed to be Gaussian with zero mean and standard deviation of 1 ºC. This assumption is based on the procedure used to calibrate the thermocouple [55], which is addressed in the experimental section.

A critical issue in Bayesian statistics is its inherent subjectivity to prior data. Whether previous information about **P** is available, it should be introduced into the PDF. In this context, whether a Gaussian distribution is considered, the prior density function can be expressed as follows:

$$\pi(\mathbf{P}) = \frac{1}{(2\pi)^{M/2}|\mathbf{V}|^{1/2}} exp\left\{-\frac{1}{2}[\mathbf{P} - \boldsymbol{\mu}]^{\mathrm{T}}\mathbf{V}^{-1}[\mathbf{P} - \boldsymbol{\mu}]\right\} \tag{20}$$

where M is the number of parameters to be estimated; $\boldsymbol{\mu}$ and $\mathbf{V}$ are the mean and covariance matrices for **P**, respectively. Matrix **V** is computed as:

$$\mathbf{V} = \begin{bmatrix} \sigma_A^2 & 0 & 0 & 0 \\ 0 & \sigma_B^2 & 0 & 0 \\ 0 & 0 & \sigma_C^2 & 0 \\ 0 & 0 & 0 & \sigma_D^2 \end{bmatrix} \tag{21}$$

By contrast, if **P** is unknown and there is no previous knowledge about it in advance, Bayes' postulate states that $\pi(\mathbf{P})$ should be a uniform distribution. Uniform prior distributions are improper, and sometimes noninformative. Proper posteriors can often be found from improper priors. Nevertheless, improper priors can lead to problems when dealing with a continuous parameter space. Thus, Jeffreys' priors, which are constructed to be "minimally acceptable" noninformative priors, can be used as reference priors [57]. For a uniform prior density function as reference assumption, $\pi(\mathbf{P}) \propto 1$ and the PPDF is then summarized as $\pi(\mathbf{Y}|\mathbf{P})$. This means that the posterior probability density becomes equal to the likelihood function, i.e., $\pi(\mathbf{P}|\mathbf{Y}) \propto \pi(\mathbf{Y}|\mathbf{P})$.

Finally, by replacing Equations (17) and (20) into Bayes' theorem, one can obtain this general formulation:

$$\ln\left[\pi(\mathbf{P}|\mathbf{Y})\right] \propto -\frac{1}{2}\left[(\mathrm{M}+\mathrm{D})\ln 2\pi + \ln|\mathbf{W}| + \ln|\mathbf{V}| + S_{MAP}(\mathbf{P})\right] \tag{22}$$

where:

$$S_{MAP}(\mathbf{P}) = [\mathbf{Y}-\mathbf{T}(\mathbf{P})]^{\mathrm{T}}\mathbf{W}^{-1}[\mathbf{Y}-\mathbf{T}(\mathbf{P})] + [\mathbf{P}-\boldsymbol{\mu}]^{\mathrm{T}}\mathbf{V}^{-1}[\mathbf{P}-\boldsymbol{\mu}] \tag{23}$$

It can be noted from Equation (23) that the estimation procedure develops into an optimization problem, in which the point estimates for **P** are achieved at the maximum of the posterior probability density (MAP – the maximum *a posteriori*). Therefore, despite using MH-MCMC to solve the inverse problem being studied, the estimation procedure could be performed by maximizing the posterior distribution, based on minimizing the maximum *a posteriori* objective function S_{MAP}. The first and second terms expressed on the right side of Equation (23) denote the trade-off between the likelihood and prior distributions, respectively, when estimating parameters by Bayesian inference. As stated earlier, all terms related to the prior distribution are set to 1 when a uniform prior model is injected into the estimation formulation. For smooth nonlinear but differentiable problems, like the one at hand, the MAP estimation problem can be solved using gradient-based optimization. MAP estimates were not used here because although they are generally fast and simple to compute, they do not provide statistical information about the estimates. For this purpose, MCMC sampling methods are usually recommended since they can easily make available information to calculate the uncertainty inherent to the posterior distribution.

2.6 Sensitivity analysis

An analysis of the sensitivity coefficients before carrying out experiments leads to a better experimental design when estimating unknown parameters. It provides guidance on how well-designed the experimental arrangement is and assesses the influence of each design variable on the mathematical model response [49]. Sensitivity analysis can also help to reduce ill-posedness and decrease experimental uncertainties. Sensitivity coefficients may seem more significant in classical gradient-based methods since they directly influence the topology of the objective function to be minimized. They are also necessary when building the sensitivity matrix to compute the estimates. However, sensitive information is also essential and needs to be analyzed when using stochastic-based methods. This is due to the fact that the sensitivity coefficients provide knowledge of the function behavior, guiding search and coverage of metaheuristics and impacting the Bayesian posterior distribution equilibrium. Thus, overall, a temperature response that is sensitive to the unknown parameter being estimated is always physically essential for understanding, formulating, and solving inverse problems [7].

Sensitivity coefficients assess the sensitivity of the temperature in relation to a change in the thermal parameter analyzed. A small sensitivity magnitude value denotes that large changes in the parameter result in small changes in the temperature field [4]. Estimating this parameter from temperature measurements is consequently difficult in such a case because the inverse problem is ill-conditioned. There is also ill-conditioning if the sensitivity coefficients are linearly dependent, or in other words, if one of the sensitivities is some combination of the others. Scaled sensitivity coefficients with large magnitudes that are linearly independent (uncorrelated) are needed for a reliable and accurate simultaneous parameter estimation [7]. The scaled sensitivity coefficient (*J*), which presents units of temperature, is the first partial derivative of the temperature *T* in relation to the parameter of interest *P* (i.e., *A, B, C* and *D*) multiplied by the parameter itself: $J_P = P \times \partial T / \partial P$. For the 1D formulation, comparing different sensitivity plots using scaled sensitivity coefficients is more convenient because it provides sensitivities on the same basis. Nevertheless, sometimes even with modified sensitivity coefficients, it may be difficult to draw conclusions about the optimal conditions to evaluate the desired parameters. It is still more difficult when dealing with various parameters and several locations since lot of data must be examined graphically. This condition, which is the case of the 3D formulation, requires a straightforward criterion to assess the sensitivity.

The D-optimality concept has been successfully employed as an experimental design method to investigate the optimal aspects in heat transfer [58]. This criterion is formulated on the maximization of the determinant Δ of the information matrix $\mathbf{X}^{\mathrm{T}}\mathbf{X}$, which is constructed from the sensitivity matrix $\mathbf{X}$ and its transpose, as follows:

$$\Delta \equiv |\mathbf{X}^{\mathrm{T}}\mathbf{X}| \tag{24}$$

$$\mathbf{X} = \frac{\partial \mathbf{T}^{\mathrm{T}}}{\partial \mathbf{P}} \tag{25}$$

$$J_P = P \frac{\partial T}{\partial P} \tag{26}$$

where $\mathbf{X} = \partial \mathbf{T}^{\mathrm{T}} / \partial \mathbf{P}$ is the sensitivity matrix of $\mathbf{T}$ with respect to $\mathbf{P}$. So, the solution of the direct problem is needed to evaluate matrix $\mathbf{X}$. The inputs of this matrix are the first partial derivatives of the dependent variable $\mathbf{T}$, which is taken for each time and sensor location, in relation to the independent variable $\mathbf{P}$, which contains the parameters that are the target of the estimation technique proposed here.

This computationally efficient criterion provides guidance for experimental designs when dealing with high-dimensional problems, which require that a small number of sensors be used to accomplish the inverse solution, for practical reasons. Moreover, it is already known that k and c_p have linearly independent sensitivity coefficients for metallic materials. Thus, the D-optimality criterion is suitable for use in this study. Therefore, from the preliminary sensitivity analysis, one can evaluate which locations in the thermal model can contribute to more sensitive temperature measurements, resulting in better conditions for the simultaneous estimation of the thermal conductivity and specific heat of the metal slab. The sensitivity computation is carried out from the properties at room temperature obtained from Valencia and Quested [24]. While temperature dependence conducts to slightly different sensitivity values when carrying out the simultaneous estimation, this analysis seeks to furnish prior knowledge regarding the feasibility of the procedure. Additionally, Bayesian computation can also be employed to investigate how the thermocouple location affects the reliability region of the inverse solution. It is rather difficult to analytically analyze the thermocouple location effect on the PPDF. Therefore, this alternative method explores and reveals the effect of the sensor location by performing numerical simulations with data from different locations and comparing the posterior estimates (both point estimates and probability limits) from MCMC samples. This is another option to guide optimal experiment design in data-driven inverse heat conduction problems to obtain accurate solutions [56].

2.7 Experimental aspects

The location of temperature sensors is essential to evaluate an inverse thermal problem since it is necessary to convey a sufficiently complete information about the transient behavior of the thermal model. Additionally, in data-driven inverse problems, it is important to achieve an accurate inverse solution using a minimum number of sensors, from a practical sense.

For high-conductivity materials, sensitivity coefficients are normally higher near heated regions. This means that better sensitivity would be obtained at the surface points under the heater. However, it is often not feasible to measure temperature at these locations using thermocouples, since the sensor strongly impacts the heater placement, leading to losses in heat transfer between the heater and metal. Embedded thermocouple wires need that some filler material to be introduced into a milled hole, which causes a discontinuity effect [59]. In this context, only the bottom surface can be explored to collect temperature data with wire thermocouples in the 1D thermal model [60]. Being the bottom surface the only point that can be explored to collect temperature, data from the 1D experiment was measured at $x = L$. Researchers have already shown that this location can transmit information that is sensitive enough to carry out the estimation process, given appropriate initial values [31], [60].

For the 3D formulation, a D-optimality-based sensitivity analysis was carried out to identify the most sensitive zones. Figure 2 shows a representation of the D-optimality criterion for all sample surfaces. The best regions for placing sensors are those that have greater values. An analysis of Figure 2 reveals that some zones of surfaces I, II, III and VI have D-criterion values with the same order of magnitude. However, as already said, when designing experiments for data-driven inverse heat conduction problems, it is of practical importance to make use of a minimum quantity of sensors to obtain a reliable, accurate inverse solution. Thus, taking into consideration the sensitivity analysis and experimental aspects (e.g., insulation deficiency), a single thermocouple was placed on the bottom surface (VI, $z = c$) at position (2.00, 2.00, $c = 8.90$) mm and welded with the aid of a capacitive discharge. Furthermore, from a practical aspect, it is worth mentioning that measuring temperature by a thermocouple at the heated surface (I, $z = 0$) is not feasible for metallic materials.

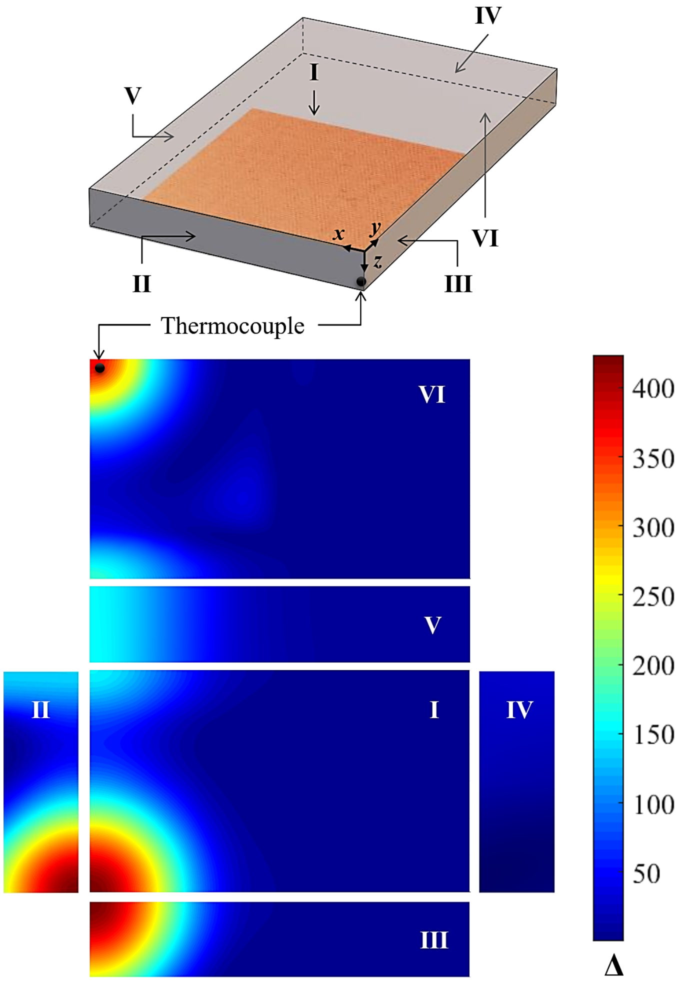

Figure 2. D-optimality criterion for all sample surfaces. Unfolded view with the sensor location.

Since the location of a single sensor in each experiment is a sensitive issue for the estimation procedure, the scaled sensitivity coefficients obtained by combining complementary thermal models must be examined. Figure 3 shows the scaled sensitivity coefficients for the 1D (J_{1D}) and 3D (J_{3D}) thermal models, and for their combination (J_{1D+3D}). One can note in this figure that complementary data increases the sensitivity coefficients of parameters C and D, corresponding to c_p, over the entire experiment. It is hard to obtain temperature data that is sufficiently sensitive to thermal conductivity when studying metals in transient state. This is because k has its sensitivity proportional to the imposed heat load, and substantially high heat flux intensities are difficult to achieve experimentally. Due to its lower sensitivity, thermal conductivity is usually more affected by measurement errors, i.e., k is more imprecisely estimated compared to c_p. Thus. more importantly, complementary experiments increase the sensitivity coefficients of parameters related to k, i.e., A and B, at the beginning of the experiments. Although low sensitivity at initial stages is generally overcome later for well-designed whole domain estimations, its effects cannot be completely neglected, since regions with sensitivity deficiency can bias or even disable the estimation procedure [4]. It is difficult to evaluate estimations using temperature data from these regions, since they are very susceptible to errors. One can conclude that it is impossible to simultaneously identify all sought-after parameters if one only considers temperature measurements during the initial moments. One can also observe that combining temperature data provides uncorrelated sensitivity coefficients with good magnitudes over time. When estimating two or more parameters, one should attempt to achieve the largest value of the determinant of the information matrix, i.e., $\Delta = \max\left|\mathbf{X}^{\mathrm{T}}\mathbf{X}\right|$. These are, respectively, the optimality criterion Δ for the 1D and 3D thermal models, and the combination of the two: 2.378×10^{8}, 5.838×10^{9}, and 3.991×10^{12}. One can see that there is a significant increase of 3 orders of magnitude in Δ when using complementary data. Even though the determinants of $\mathbf{X}_{1\mathrm{D}}^{\mathrm{T}}\mathbf{X}_{1\mathrm{D}}$ and $\mathbf{X}_{3\mathrm{D}}^{\mathrm{T}}\mathbf{X}_{3\mathrm{D}}$ can be null, the determinant of the sum $\mathbf{X}_{1\mathrm{D}}^{\mathrm{T}}\mathbf{X}_{1\mathrm{D}}+\mathbf{X}_{3\mathrm{D}}^{\mathrm{T}}\mathbf{X}_{3\mathrm{D}}$ is unlikely to be equal to zero. In this sense, the minimum hypervolume obtained from Equation (24) is defined by the maximum of the determinant of $\mathbf{X}_{1\mathrm{D}}^{\mathrm{T}}\mathbf{X}_{1\mathrm{D}}+\mathbf{X}_{3\mathrm{D}}^{\mathrm{T}}\mathbf{X}_{3\mathrm{D}}$ [44]. Since the purpose of sensitivity evaluations is to obtain prior knowledge about the inverse procedure feasibility, one can be assured that combining the collected measurements will greatly improve sensitivity and enable a suitably accurate inverse solution.

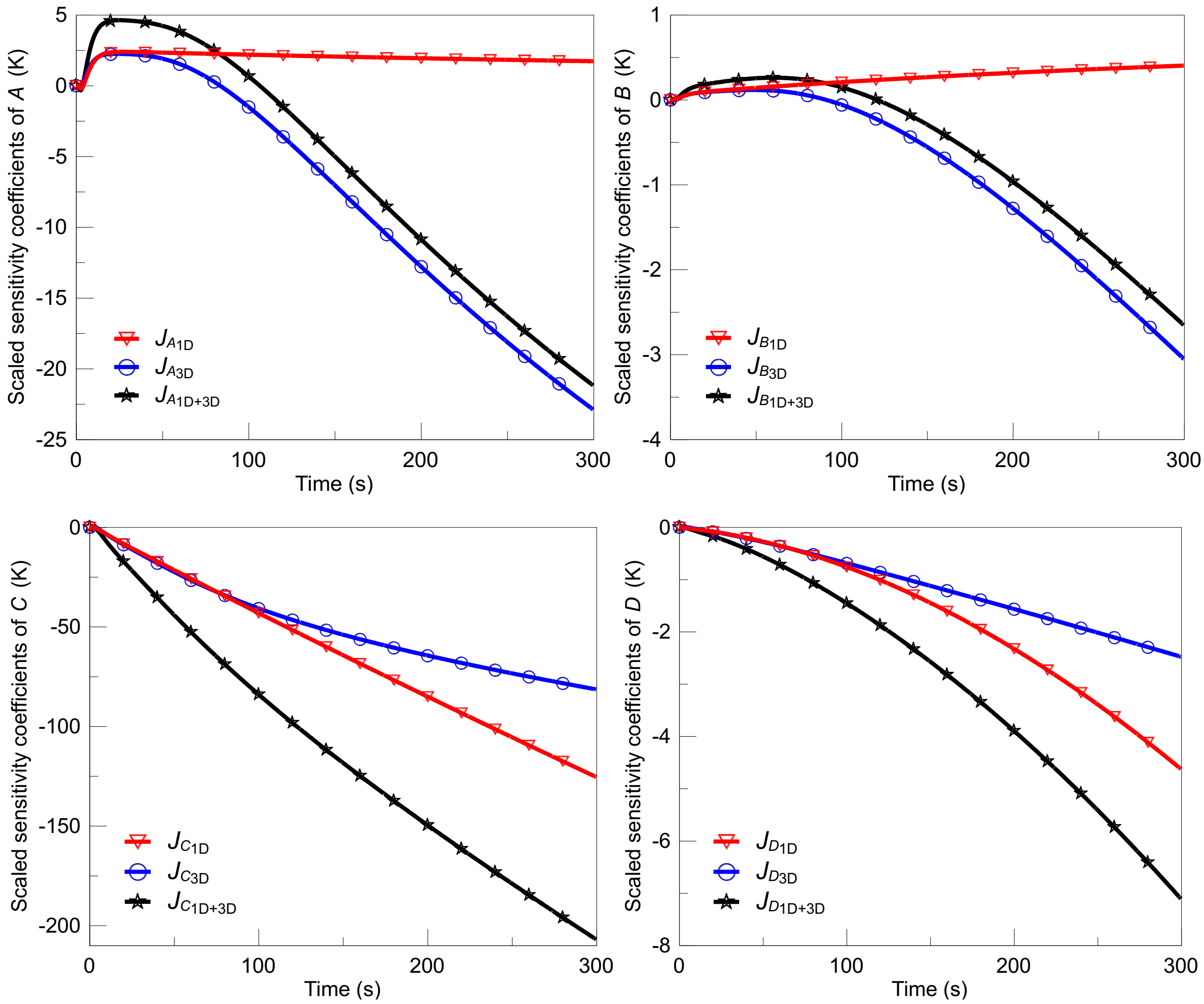

Figure 3. Scaled sensitivity coefficients of parameters describing the linear functions of $k(T)$ and $c_p(T)$.

2.8 Heat conduction experiments

Both experimental arrangements are somewhat similar and include: a metal plate with the top surface exposed to a constant heat flux, while the side and bottom surfaces were thermally insulated; a resistive heater (Omega SRFGA20210, 333.6 Ω); two insulation blocks made up of refractory ceramic fiber ($k = 0.05$ W m^{-1} K^{-1} and $c_p = 865$ J kg^{-1} K^{-1}, at room temperature); a T-type thermocouple; a programmable digital DC power supply (IT6953A, least counts 1 mA, 1 mV); two digital multimeters (Minipa ET2042C, resolution ± 0.1 Ω, ± 0.01 A); a data acquisition system (DAS Keysight 34980A); and a computer. Figure 4 shows a representation of the experimental setups used to thermally characterize 304 austenitic stainless steel.

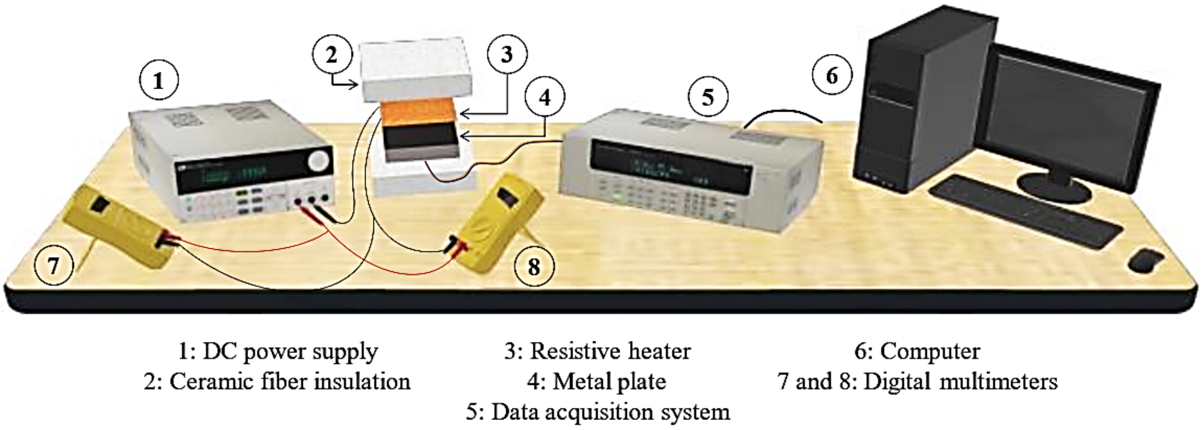

Figure 4. Schematic of the experimental arrangement used to simultaneously identify $k(T)$ and $c_p(T)$.

The test samples were milled and ground to the following dimensions (unit: mm): 49.95 width (a), 50.05 length (b), and 10.70 thickness (c), for the 1D experiment; and 60.30 width (a), 99.80 length (b), and 8.90 thickness (c), for the 3D experiment. These dimensions were assessed with a vernier caliper (Mitutoyo 530104BR, resolution ± 0.05 mm). The sample weights were taken by a precision balance (Bel S2202H, resolution ± 0.1 g) and divided by the volumes, determining the mean density at 8024 kg m^{-3}. The chemical composition of the 304 ASS specimens, which was determined using an XRF spectrometer (Niton XL3t-800), is as follows (in wt.%): 0.07C-18.5Cr-1.7Mn-9.3Ni-0.8Si-0.03P-0.03S-0.2Cu-Fe.

The specimens were placed in a pocket milled into the bottom insulation block, and initially kept at room temperature. They were heated for 300 s, reaching a temperature around 150 ºC at the thermocouple location. Electric power was conducted to the heater by the digital

DC power supply, and both current and voltage were measured by the digital multimeters. Both experiments were performed using a heat flux input of 20000 W m^{-2} maintained constant during the entire duration of the tests, until power was switched off. Transient temperature measurements were collected at 0.1-sec intervals by the DAS, recorded, and then used as information to perform the simultaneous parameter estimation in the desktop computer. The thermocouples used (30AWG with resolution of ± 0.1 ºC, and diameter of 0.25 mm) were calibrated by comparing their readings with measurements from a PT-100 sensor in a thermostatic bath (Marconi MA184, resolution ± 0.01 ºC), and welded on the samples using capacitive discharge resistance welding.

One had to measure several physical quantities related to the experimental setups and introduce these into COMSOL Multiphysics to determine the contact resistance, which was 0.0010 K m^2 W^{-1} for the 1D experiment and 0.0012 K m^2 W^{-1} for the 3D experiment. A digital roughness meter (Mitutoyo SJ210, resolution ± 0.01 μm) measured surface roughness at 0.18 μm for the 1D plate, 0.21 μm for the 3D plate, and 0.83 μm for the resistive heater. Contact pressure between the heater and the specimen was assessed by dividing the test setup weight by its cross-sectional area. Contact pressure was 1411.7 N m^{-2} and 1293.3 N m^{-2} for the 1D and 3D experiments, respectively. Hardness was determined with a hardness testing machine (Otto Wolpert-Werke Testor HT1, resolution of ± 0.5 HB), resulting in 125.5 HB for the 1D sample and 128.0 HB for the 3D sample.

2.9 Results and discussion

For any numerical simulation, the computed solution must be independent of the mesh size. Mesh independence assessments were performed for both thermal models by solving their direct problems. For the 1D model, mesh geometries with 5, 8, 11, 14, and 17 elements were tested. Differences close to 0.003 ºC were noted among the results using meshes with 11 and 14 elements. In the 3D model, temperature distribution was computed in COMSOL using five pre-defined mesh geometries, which were extremely-fine, extra-fine, fine, normal, and coarse. These were generated directly by the default meshing options and were adapted to the characteristics of the thermal problem. Differences no greater than 0.009 ºC were noted between the results obtained with these meshes. Therefore, to obtain an accurate inverse solution at reasonable computational costs, when simultaneously identifying the sought thermal properties, the 11-element mesh was used to solve the 1D problem, and the “coarse" mesh was used to evaluate the 3D problem.

To assess the Bayesian estimation methodology, the total number of states (G) was set to 8000, which is enough to avoid the oscillation of the initial samples dealt with by the Markov chain with a reasonably fast computational rate. As the MCMC algorithm is not initialized at its stationary distribution, there may be some bias caused by its starting points. To compensate for this, the conception of burn-in period was introduced to reduce the effect of correlation between the initial MCMC samples on estimation results. This implies that some states (iterations) at the beginning of the MCMC run are eliminated, with the number of discarded states being chosen to be great enough for the MCMC chain to reach its invariant distribution by this time. Figure 5 shows the evolution of the natural logarithm of the PPDF $\ln[\pi(\mathbf{P}|\mathbf{Y})]$ as a function of the number of states of the Markov chain for the MCMC run using uniform prior and 8000 states. In this figure, it can be observed that the Markov chain converges reaching equilibrium in approximately 4000 states. Since the effect of the MCMC initial condition has suitably been dissipated, the first 4000 states of the MH-MCMC were disregarded for the statistical computation of the estimates.

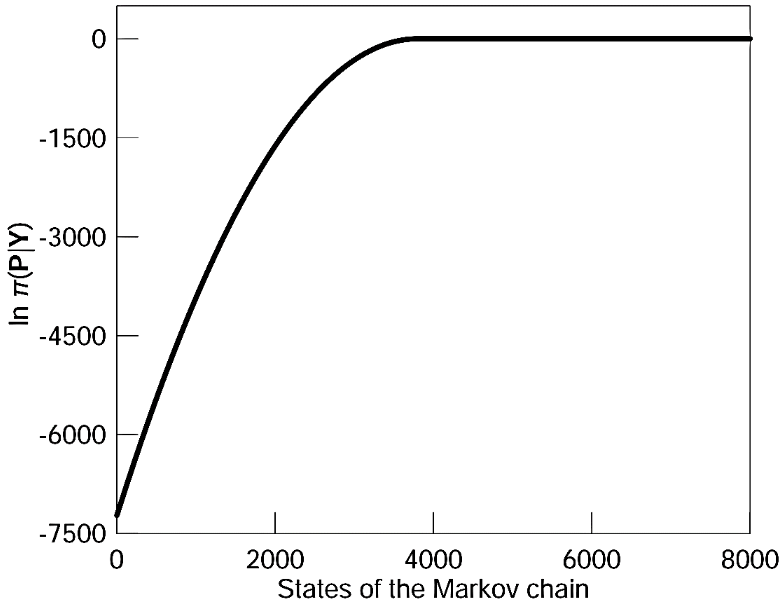

Figure 5. Evolution of the PPDF versus the number of states of the Markov chain.

To solve the inverse problem here and guarantee convergence of the estimation process, a key point is that suitable prior knowledge about the sought-after parameters is needed. Generally, normally distributed models and uniformly distributed models are used as prior information. Inserting subjective prior information is a fundamental principle of the Bayesian framework that introduces bias in the estimation results, since this statistical-based method is easily affected by the initial guesses (prior distribution). The uniform distribution with probability density of $\pi(A) \sim U(0, 24)$ W m^{-1} K^{-1}, $\pi(B) \sim U(0, 0.02)$ W m^{-1} K^{-2}, $\pi(C) \sim U(0, 700)$ J kg^{-1} K^{-1}, and $\pi(D) \sim U(0, 0.2)$ J kg^{-1} K^{-2} was assumed as prior and feasible search space. Analyzes were conducted to attempt to enlarge the search limits, but the outcomes were severely impacted when using wider search regions. Uniform priors enable accurate results with a reasonable computational cost, since some calculations are simplified when this kind of prior is used.

Table 1 shows the results of the simultaneous Bayesian estimation for five sets of complementary experiments. This means that measurements were replicated at least five times for each specimen. The standard deviation values denote the probability uncertainty inherent to Bayesian statistics. The average of the Bayesian estimates was used to construct linear curves describing k and c_p versus temperature, as shown in Figures 6 and 7. These thermal property correlation equations, Equations (27)-(28), can be applied to temperatures ranging from 20 ºC to 150 ºC. Four significant digits were used to specify the parameters of interest, due to the number of significant figures of the less accurate quantity experimentally measured, namely the roughness measurement. Comparing the linear functions for $k(T)$ and $c_p(T)$ obtained in this study and literature data, it can be seen that the slopes of the k linear functions are very similar for all studies, which is not the case with c_p. In this sense, it is worthwhile to mention that variations may occur mainly due to differences in the thermal characterization methods used and in the chemical composition of the stainless steel investigated in this study and those studied elsewhere. For simplicity, since the behaviors are very similar, only the graphical results corresponding to the PPDFs of *A, B, C,* and *D* for the first experimental set are shown in Figure 8.

Table 1. Simultaneous estimation of k and c_p parameters for 304 austenitic stainless steel.

Set	Bayesian estimated values							
	A [W m^{-1} K^{-1}]		B [W m^{-1} K^{-2}]		C [J kg^{-1} K^{-1}]		D [J kg^{-1} K^{-2}]	
	Mean	SD	Mean	SD	Mean	SD	Mean	SD
1	13.91	0.30	0.01369	0.00039	493.5	11.7	0.1465	0.0028
2	13.28	0.27	0.01406	0.00045	489.3	12.8	0.1422	0.0032
3	14.01	0.35	0.01469	0.00040	494.0	12.4	0.1389	0.0026
4	14.33	0.31	0.01348	0.00042	490.9	12.0	0.1451	0.0029
5	13.80	0.29	0.01353	0.00037	489.8	12.5	0.1395	0.0029

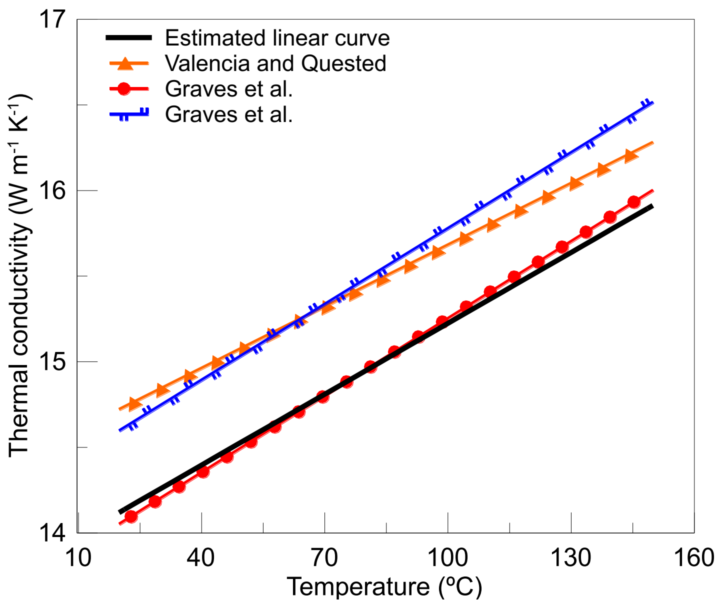

Figure 6. Temperature-dependent thermal conductivity of 304 austenitic stainless steel. Comparison of the lines determined in this study with curves reported in Valencia and Quested [24] and Graves et al. [61].

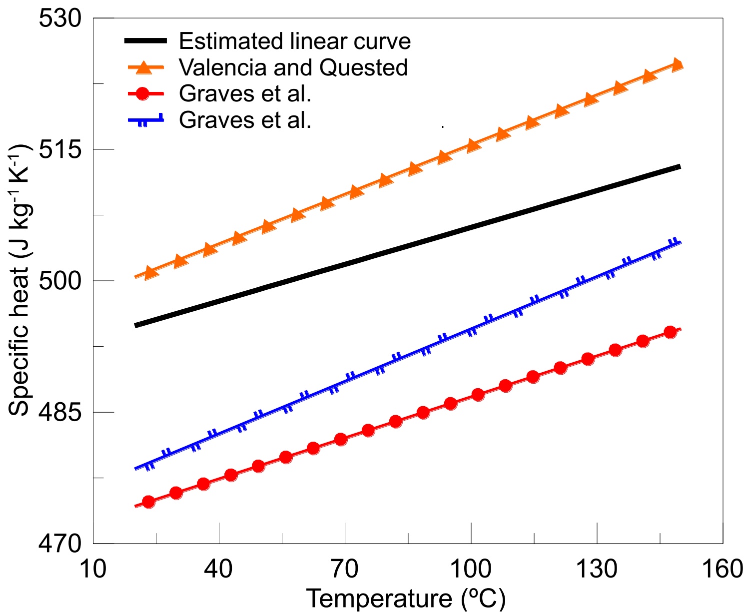

Figure 7. Temperature-dependent specific heat of 304 austenitic stainless steel. Comparison of the lines determined in this study with curves reported in Valencia and Quested [24] and Graves et al. [61].

$$k(T) = 13.84 + 0.01380 \times T \; [\mathrm{W\ m^{-1}\ K^{-1}}] \tag{27}$$

$$c_p(T) = 492.0 + 0.1402 \times T \; [\mathrm{J\ kg^{-1}K^{-1}}] \tag{28}$$

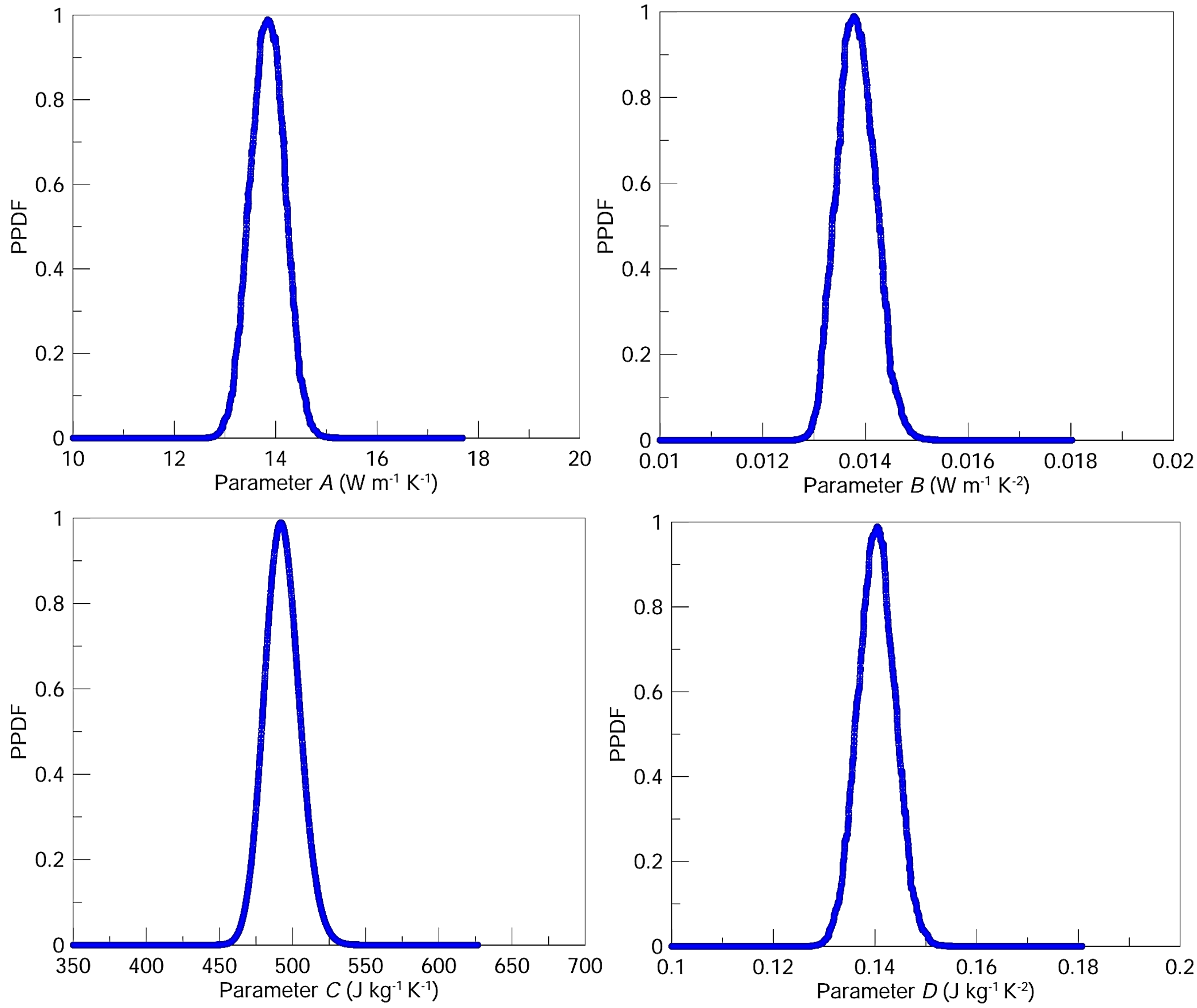

Figure 8. PPDFs of the estimated parameters for the first experimental set.

Ideally, the differences between the measured temperature and the corresponding calculated temperature are desirable to be close to zero, but that is impractical. Any object, warmer than its surroundings, naturally loses a portion of its thermal energy. Since the ceramic fiber insulation has non-null thermal properties, some heat loss is unavoidable, causing some variations in the heat flux. This means that the actual heat flux load is time-varying, rather than constant. As a result, the mathematical modeling of the physical problem is somewhat imperfect. Figure 9 shows a comparison between the measured temperatures of the first set of complementary experiments and the corresponding temperatures computed with the estimated curves. One can observe that the model-predicted temperature histories and the experimentally measured temperatures match well for both thermal models. The largest residuals for the 1D and 3D formulation were 2.36 ºC and 3.03 ºC, in absolute values, respectively. These differences are acceptable because they represent approximately 1.8% and 2.5% of the maximum temperature variation, in a relative sense. This condition can be regarded as acceptable especially because one deals with a low-cost experimental setup in a transient state. Thus, unmodeled heat loss and inconsistencies involved in the inverse approach are proved to be minimal, indicating the adequacy of the thermal models used.

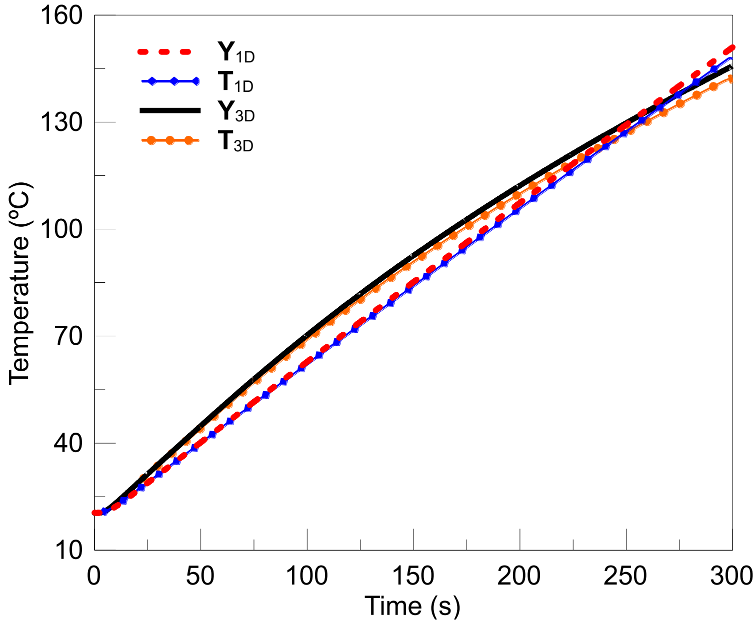

Figure 9. Temperature histories for the 1D and 3D thermal models. Comparison of measurements with numerically computed temperatures.

As part of the validation process, the repeatability of the estimation results is evaluated by performing the inverse retrieval of the heat flux intensity imposed, based on the estimated linear curves. The measured temperature data and lines estimated for the thermal properties are employed to retrieve the applied heat flux using Beck's nonlinear formulation with 10 future time steps [4]. Figure 10 shows a comparison between retrieved heat flux histories. An analysis of this figure reveals that the heat fluxes agree well with the experimental heat load of 20000 W m^{-2}.

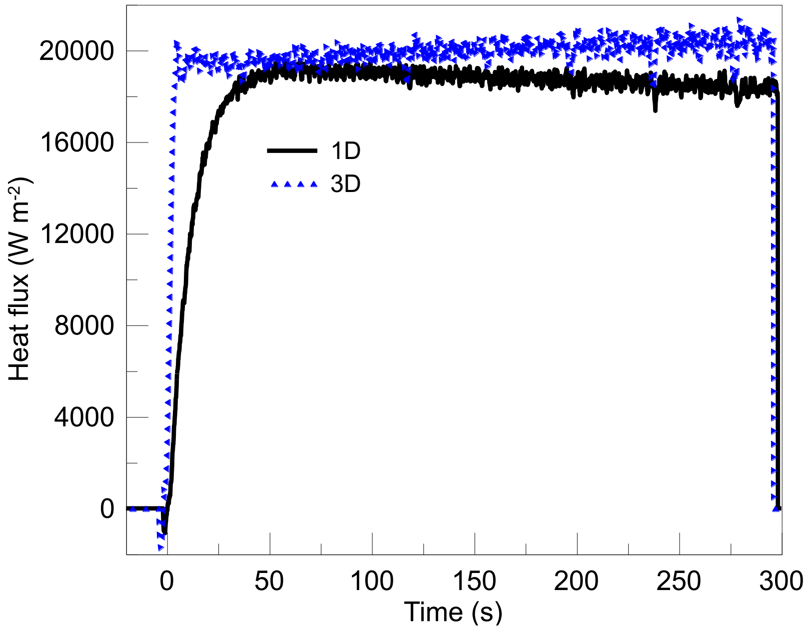

Figure 10. Comparison between the retrieved heat flux histories.

2.10 Summary

This first case study focused on using complementary experiments to simultaneously identify parameters describing the linearly temperature-dependent thermal conductivity and specific heat of 304 austenitic stainless steel. Inverse thermal analysis was based on combining measurements from two transient experiments conducted at room temperature, where each had a single sensor. Sensitivity analysis showed that complementary temperature measurements increased the sensitivity coefficients of parameters for c_p, and raised those for k at the initial stages, where lack of sensitivity is critical when handling metals. These more sensitive data produced a significant increase in the determinant of the information matrix, resulting in improved estimates. Bayesian inference was used to take advantage of this additional sensitive information. Single-step estimation of temperature-dependent parameters was carried out considering measurement data corresponding to the entire temperature domain. As this study used a statistical optimization approach, probability distributions were obtained for the estimates instead of fixed values. Despite showing its well-known behavior of being sensitive to the prior information inserted into the statistical estimator, the Bayesian uncertainties had relatively small values, indicating the reliability of the results.

Future research work should focus on applying the proposed technique to different metallic materials, subjected to heat treatments. Additionally, as the current experimental setup provides reliable k and c_p estimates up to 150 ºC, obtaining an experimental setup capable of handling higher temperature ranges would be important.

3. Appendix

3.1 Publications

- Ramos N P, Antunes M M, and Lima e Silva S M M (2023). *A heat flux-corrected experimental inverse technique for simultaneously estimating the thermal properties of a metallic medium as functions of temperature*. **Experimental Heat Transfer**. DOI 10.1080/08916152.2023.2189328.
- Ramos N P, Antunes M M, Silva A A A P, and Lima e Silva S M M (2023). *Effects of tempering temperature on temperature-dependent thermal properties of 1045 steel*. **Journal of Materials Science** 58 1905–1924. DOI 10.1007/s10853-022-08137-0.
- Ramos N P, Antunes M M, and Lima e Silva S M M (2022). *Complementary transient thermal models and metaheuristics to simultaneously identify linearly temperature-dependent thermal properties of austenitic stainless steels*. **Physica Scripta** 97(11) 115006. DOI: 10.1088/1402-4896/ac99ac.
- Ramos N P, Antunes M M, Guimarães G, and Lima e Silva S M M (2022). *Simultaneous Bayesian estimation of the temperature-dependent thermal properties of a metal slab using a three-dimensional transient experimental approach*. **International Journal of Thermal Sciences** 179 107671. DOI: 10.1016/j.ijthermalsci.2022.107671.
- Ramos N P, Antunes M M, and Lima e Silva S M M (2021). *An experimental and straightforward approach to simultaneously estimate temperature-dependent thermophysical properties of metallic materials*. **International Journal of Thermal Sciences** 166 106960. DOI: 10.1016/j.ijthermalsci.2021.106960.

- Ramos N P, Carollo L F S, and Lima e Silva S M M (2020). *Contact resistance analysis applied to simultaneous estimation of thermal properties of metals*. **Measurement Science and Technology** 31(10) 105601. DOI 10.1088/1361-6501/ab8e6a.

3.2 Ongoing papers

- Ramos N P, Antunes M M, Abreu L A P, Faco H, and Lima e Silva S M M. Simultaneous estimation of effective temperature-dependent thermal properties of glass fiber-reinforced polymer for air-core reactor insulation via inverse approach.
- Ramos N P, Buenrostro L D, Lima e Silva S M M, and Gosselin L. Simultaneous estimation of hygrothermal properties of a prefabricated lightweight wall using one-year on-site measurements to solve inverse problems.
- Ramos N P, Buenrostro L D, Lima e Silva S M M, and Gosselin L. Inverse estimation of the annual heat flux through the internal surface of a multilayer wall in an occupied prefabricated house from field measurements.
- Ramos N P, Antunes M M, Silva A A A P, Guimarães G, and Lima e Silva S M M. Influence of quenching and tempering heat treatment on the heat flux to the workpiece in dry milling of AISI 1045 steel.

3.3 Thermal property measurements

- Measurement of the thermal conductivity of a skin cream using the hot-wire method for the company InoxNews.

- Measurement of the thermal conductivity of composite materials using the hot-plate method for the company General Electrics.

3.4 Sandwich PhD

From August 2022 to May 2023, PhD internship at the Thermal Energy Transfer laboratory at Université Laval, under the supervision of Professor Louis Gosselin. The research internship focused on applying inverse heat and moisture analysis to investigate the hygrothermal behavior of building walls and their materials.

4. References

[1] J. Hadamard, *Lectures on Cauchy's Problem in Linear Partial Differential Equations*. Yale University Press, 1923.

[2] O. M. Alifanov, *Inverse Heat Transfer Problems*. in International Series in Heat and Mass Transfer. Berlin, Heidelberg: Springer Berlin Heidelberg, 1994. doi: 10.1007/978-3-642-76436-3.

[3] O. M. Alifanov, "Solution of an inverse problem of heat conduction by iteration methods," *Journal of Engineering Physics*, vol. 26, no. 4, pp. 471–476, Apr. 1974, doi: 10.1007/BF00827525.

[4] K. A. Woodbury, Ed., *Inverse Engineering Handbook*. CRC Press, 2002. doi: 10.1201/9781420041613.

[5] B. Czél, K. A. Woodbury, and G. Gróf, "Simultaneous estimation of temperature-dependent volumetric heat capacity and thermal conductivity functions via neural networks," *Int J Heat Mass Transf*, vol. 68, pp. 1–13, Jan. 2014, doi: 10.1016/j.ijheatmasstransfer.2013.09.010.

[6] F. Pierron and S. Avril, "Experimental Mechanics - Inverse Problems in Experimental Solid Mechanics," in *Mechanical Engineering, Energy Systems and Sustainable Development -Volume V*, EOLSS Publications, 2009.

[7] M. N. Özisik and H. R. B. Orlande, *Inverse Heat Transfer*. Routledge, 2018. doi: 10.1201/9780203749784.

[8] J. L. J. Pereira, M. B. Francisco, C. A. Diniz, G. Antônio Oliver, S. S. Cunha, and G. F. Gomes, "Lichtenberg algorithm: A novel hybrid physics-based meta-heuristic for global optimization," *Expert Syst Appl*, vol. 170, p. 114522, May 2021, doi: 10.1016/j.eswa.2020.114522.

[9] X. S. Yang, "Review of meta-heuristics and generalised evolutionary walk algorithm," *International Journal of Bio-Inspired Computation*, vol. 3, no. 2, p. 77, 2011, doi: 10.1504/IJBIC.2011.039907.

[10] M. F. Tabassum *et al.*, "Optimal solution of engineering design problems through differential gradient evolution plus algorithm: a hybrid approach," *Phys Scr*, vol. 97, no. 1, p. 014002, Jan. 2022, doi: 10.1088/1402-4896/ac41ec.

[11] G. C. V. Ramadas, E. M. G. P. Fernandes, A. M. V. Ramadas, A. M. A. C. Rocha, and M. F. P. Costa, "On Metaheuristics for Solving the Parameter Estimation Problem in Dynamic Systems: A Comparative Study," *Journal of Optimization*, vol. 2018, pp. 1–21, 2018, doi: 10.1155/2018/3213484.

[12] Y. Jannot and A. Degiovanni, *Thermal Properties Measurement of Materials*. Wiley, 2018. doi: 10.1002/9781119475057.

[13] L. Gosselin, M. Tye-Gingras, and F. Mathieu-Potvin, "Review of utilization of genetic algorithms in heat transfer problems," *Int J Heat Mass Transf*, vol. 52, no. 9–10, pp. 2169–2188, Apr. 2009, doi: 10.1016/j.ijheatmasstransfer.2008.11.015.

[14] J. P. Kaipio and C. Fox, "The Bayesian Framework for Inverse Problems in Heat Transfer," *Heat Transfer Engineering*, vol. 32, no. 9, pp. 718–753, Aug. 2011, doi: 10.1080/01457632.2011.525137.

[15] J. Berger, H. R. B. Orlande, N. Mendes, and S. Guernouti, "Bayesian inference for estimating thermal properties of a historic building wall," *Build Environ*, vol. 106, pp. 327–339, Sep. 2016, doi: 10.1016/j.buildenv.2016.06.037.

[16] N. Gnanasekaran and C. Balaji, "A Bayesian approach for the simultaneous estimation of surface heat transfer coefficient and thermal conductivity from steady state experiments on fins," *Int J Heat Mass Transf*, vol. 54, no. 13–14, pp. 3060–3068, Jun. 2011, doi: 10.1016/j.ijheatmasstransfer.2011.01.028.

[17] P. Pasquier and D. Marcotte, "Robust identification of volumetric heat capacity and analysis of thermal response tests by Bayesian inference with correlated residuals," *Appl Energy*, vol. 261, p. 114394, Mar. 2020, doi: 10.1016/j.apenergy.2019.114394.

[18] D. Lesnic, *Inverse Problems with Applications in Science and Engineering*. Boca Raton: Chapman and Hall/CRC, 2021. doi: 10.1201/9780429400629.

[19] B. Lin, Y. Chen, and G. Zhang, "Technological progress and rebound effect in China's nonferrous metals industry: An empirical study," *Energy Policy*, vol. 109, pp. 520–529, Oct. 2017, doi: 10.1016/j.enpol.2017.07.031.

[20] K. H. Lo, C. H. Shek, and J. K. L. Lai, "Recent developments in stainless steels," *Materials Science and Engineering: R: Reports*, vol. 65, no. 4–6, pp. 39–104, May 2009, doi: 10.1016/j.mser.2009.03.001.

[21] M. Naghizadeh and H. Mirzadeh, "Microstructural Evolutions During Reversion Annealing of Cold-Rolled AISI 316 Austenitic Stainless Steel," *Metallurgical and Materials Transactions A*, vol. 49, no. 6, pp. 2248–2256, Jun. 2018, doi: 10.1007/s11661-018-4583-6.

[22] N. P. Ramos, M. de Melo Antunes, A. A. A. P. da Silva, and S. M. M. de Lima e Silva, "Effects of tempering temperature on temperature-dependent thermal properties of 1045 steel," *J Mater Sci*, vol. 58, no. 4, pp. 1905–1924, Jan. 2023, doi: 10.1007/s10853-022-08137-0.

[23] J. Wilzer, F. Lüdtke, S. Weber, and W. Theisen, "The influence of heat treatment and resulting microstructures on the thermophysical properties of martensitic steels," *J Mater Sci*, vol. 48, no. 24, pp. 8483–8492, Dec. 2013, doi: 10.1007/s10853-013-7665-2.

[24] J. Valencia and P. N. Quested, “ASM Handbook, Casting - Thermophysical properties 15,” in *ASM Handbook - Casting*, ASM, 2008, pp. 468–481. doi: 10.1361/asmhba0005240.

[25] R. G. Dourado da Silva, D. C. Ferreira, F. V. Avelar Dutra, and S. M. M. Lima e Silva, “Simultaneous real time estimation of heat flux and hot spot temperature in machining process using infrared camera,” *Case Studies in Thermal Engineering*, vol. 28, p. 101352, Dec. 2021, doi: 10.1016/j.csite.2021.101352.

[26] W. Buck and S. Rudtsch, “Thermal properties - Measurement methods for materials properties,” in *Springer Handbook of Materials Measurement Methods*, H. Czichos, T. Saito, and L. Smith, Eds., Berlin, Heidelberg: Springer Berlin Heidelberg, 2006, pp. 399–428. doi: 10.1007/978-3-540-30300-8.

[27] A. Martínez, M. Carmona, C. Cortés, and I. Arauzo, “Characterization of Thermophysical Properties of Phase Change Materials Using Unconventional Experimental Technologies,” *Energies (Basel)*, vol. 13, no. 18, p. 4687, Sep. 2020, doi: 10.3390/en13184687.

[28] S. E. Gustafsson, E. Karawacki, and M. N. Khan, “Transient hot-strip method for simultaneously measuring thermal conductivity and thermal diffusivity of solids and fluids,” *J Phys D Appl Phys*, vol. 12, no. 9, pp. 1411–1421, Sep. 1979, doi: 10.1088/0022-3727/12/9/003.

[29] W. J. Parker, R. J. Jenkins, C. P. Butler, and G. L. Abbott, “Flash Method of Determining Thermal Diffusivity, Heat Capacity, and Thermal Conductivity,” *J Appl Phys*, vol. 32, no. 9, pp. 1679–1684, Sep. 1961, doi: 10.1063/1.1728417.

[30] B. Abad, D.-A. Borca-Tasciuc, and M. S. Martin-Gonzalez, “Non-contact methods for thermal properties measurement,” *Renewable and Sustainable Energy Reviews*, vol. 76, pp. 1348–1370, Sep. 2017, doi: 10.1016/j.rser.2017.03.027.

[31] N. P. Ramos, L. F. dos Santos Carollo, and S. M. M. de Lima e Silva, “Contact resistance analysis applied to simultaneous estimation of thermal properties of metals,” *Meas Sci Technol*, vol. 31, no. 10, p. 105601, Oct. 2020, doi: 10.1088/1361-6501/ab8e6a.

[32] Y. Jannot, V. Felix, and A. Degiovanni, “A centered hot plate method for measurement of thermal properties of thin insulating materials,” *Meas Sci Technol*, vol. 21, no. 3, p. 035106, Mar. 2010, doi: 10.1088/0957-0233/21/3/035106.

[33] Y. Jannot, A. Degiovanni, and G. Payet, “Thermal conductivity measurement of insulating materials with a three layers device,” *Int J Heat Mass Transf*, vol. 52, no. 5–6, pp. 1105–1111, Feb. 2009, doi: 10.1016/j.ijheatmasstransfer.2008.09.017.

[34] Y. Jannot, J. Meulemans, V. Schick, M. Capp, and I. Bargain, “A Comparative Fluxmetric (CFM) Method for Apparent Thermal Conductivity Measurement of

Insulating Materials at High Temperature," *Int J Thermophys*, vol. 41, no. 7, p. 94, Jul. 2020, doi: 10.1007/s10765-020-02676-x.

[35] J. R. Ferreira-Oliveira, L. R. R. de Lucena, R. P. B. Dos Reis, C. J. de Araújo, and C. R. Bezerra-Filho, "Thermal diffusivity measurement of stainless-steel alloys through use of the Angstrom's method," *Experimental Heat Transfer*, vol. 35, no. 4, pp. 419–439, Jun. 2022, doi: 10.1080/08916152.2021.1887407.

[36] Z. Barani *et al.*, "Thermal Properties of the Binary-Filler Hybrid Composites with Graphene and Copper Nanoparticles," *Adv Funct Mater*, vol. 30, no. 8, Feb. 2020, doi: 10.1002/adfm.201904008.

[37] T. R. Pavlov, D. Staicu, L. Vlahovic, R. J. M. Konings, P. Van Uffelen, and M. R. Wenman, "A new method for the characterization of temperature dependent thermo-physical properties," *International Journal of Thermal Sciences*, vol. 124, pp. 98–109, Feb. 2018, doi: 10.1016/j.ijthermalsci.2017.10.008.

[38] E. García, I. Amaya, and R. Correa, "Estimation of thermal properties of a solid sample during a microwave heating process," *Appl Therm Eng*, vol. 129, pp. 587–595, Jan. 2018, doi: 10.1016/j.applthermaleng.2017.10.037.

[39] F. Mohebbi, M. Sellier, and T. Rabczuk, "Estimation of linearly temperature-dependent thermal conductivity using an inverse analysis," *International Journal of Thermal Sciences*, vol. 117, pp. 68–76, Jul. 2017, doi: 10.1016/j.ijthermalsci.2017.03.016.

[40] B. Lamien *et al.*, "A Bayesian approach for the estimation of the thermal diffusivity of aerodynamically levitated solid metals at high temperatures," *Int J Heat Mass Transf*, vol. 141, pp. 265–281, Oct. 2019, doi: 10.1016/j.ijheatmasstransfer.2019.06.054.

[41] B. Sawaf, M. N. Ozisik, and Y. Jarny, "An inverse analysis to estimate linearly temperature dependent thermal conductivity components and heat capacity of an orthotropic medium," *Int J Heat Mass Transf*, vol. 38, no. 16, pp. 3005–3010, Nov. 1995, doi: 10.1016/0017-9310(95)00044-A.

[42] C.-H. Huang and Y. Jan-Yuan, "An inverse problem in simultaneously measuring temperature-dependent thermal conductivity and heat capacity," *Int J Heat Mass Transf*, vol. 38, no. 18, pp. 3433–3441, Dec. 1995, doi: 10.1016/0017-9310(95)00059-I.

[43] R. Fischer *et al.*, "The concept of Integrated Data Analysis of complementary experiments," in *AIP Conference Proceedings*, AIP, 2007, pp. 195–202. doi: 10.1063/1.2821262.

[44] R. L. McMasters, F. de Monte, and J. V. Beck, "Estimating Two Heat-Conduction Parameters From Two Complementary Transient Experiments," *J Heat Transfer*, vol. 140, no. 7, Jul. 2018, doi: 10.1115/1.4038855.

[45] Boyd and Little, "Complementary data fusion for limited-angle tomography," in *Proceedings of IEEE Conference on Computer Vision and Pattern Recognition CVPR-94*, IEEE Comput. Soc. Press, 1994, pp. 288–294. doi: 10.1109/CVPR.1994.323842.

[46] P. B. Weichman, D. R. Lun, M. H. Ritzwoller, and E. M. Lavely, "Study of surface nuclear magnetic resonance inverse problems," *J Appl Geophy*, vol. 50, no. 1–2, pp. 129–147, May 2002, doi: 10.1016/S0926-9851(02)00135-0.

[47] J. J. Led and H. Gesmar, "The applicability of the magnetization-transfer NMR technique to determine chemical exchange rates in extreme cases. The importance of complementary experiments," *Journal of Magnetic Resonance (1969)*, vol. 49, no. 3, pp. 444–463, Oct. 1982, doi: 10.1016/0022-2364(82)90257-8.

[48] Y. Cao, F. Wang, Z. He, J. Yang, and Y. Cao, "Boosting Image Super-Resolution via Fusion of Complementary Information Captured by Multi-Modal Sensors," *IEEE Sens J*, vol. 22, no. 4, pp. 3405–3416, Feb. 2022, doi: 10.1109/JSEN.2021.3139452.

[49] H. N. Mehta, P. Benyathiar, D. K. Mishra, and M. Varney, "Complementary experiments for parameter estimation in heat transfer model," *Food and Bioproducts Processing*, vol. 128, pp. 240–246, Jul. 2021, doi: 10.1016/j.fbp.2021.06.004.

[50] P. Benyathiar, K. D. Dolan, and D. K. Mishra, "Optimal Design of Complementary Experiments for Parameter Estimation at Elevated Temperature of Food Processing," *Foods*, vol. 11, no. 17, p. 2611, Aug. 2022, doi: 10.3390/foods11172611.

[51] M. Bahrami, J. R. Culham, M. M. Yananovich, and G. E. Schneider, "Review of Thermal Joint Resistance Models for Nonconforming Rough Surfaces," *Appl Mech Rev*, vol. 59, no. 1, pp. 1–12, Jan. 2006, doi: 10.1115/1.2110231.

[52] C. V. Madhusudana, "Accuracy in thermal contact conductance experiments - the effect of heat losses to the surroundings," *International Communications in Heat and Mass Transfer*, vol. 27, no. 6, pp. 877–891, Aug. 2000, doi: 10.1016/S0735-1933(00)00168-8.

[53] M. G. Cooper, B. B. Mikic, and M. M. Yovanovich, "Thermal contact conductance," *Int J Heat Mass Transf*, vol. 12, no. 3, pp. 279–300, Mar. 1969, doi: 10.1016/0017-9310(69)90011-8.

[54] J. P. Kaipio and C. Fox, "The Bayesian Framework for Inverse Problems in Heat Transfer," *Heat Transfer Engineering*, vol. 32, no. 9, pp. 718–753, Aug. 2011, doi: 10.1080/01457632.2011.525137.

[55] C. A. A. Mota, H. R. B. Orlande, M. O. M. De Carvalho, V. Kolehmainen, and J. P. Kaipio, "Bayesian Estimation of Temperature-Dependent Thermophysical Properties and Transient Boundary Heat Flux," *Heat Transfer Engineering*, vol. 31, no. 7, pp. 570–580, Jun. 2010, doi: 10.1080/01457630903425635.

[56] J. Wang and N. Zabaras, “A Bayesian inference approach to the inverse heat conduction problem,” *Int J Heat Mass Transf*, vol. 47, no. 17–18, pp. 3927–3941, Aug. 2004, doi: 10.1016/j.ijheatmasstransfer.2004.02.028.

[57] J. P. Kaipio and C. Fox, “The Bayesian Framework for Inverse Problems in Heat Transfer,” *Heat Transfer Engineering*, vol. 32, no. 9, pp. 718–753, Aug. 2011, doi: 10.1080/01457632.2011.525137.

[58] N. P. Ramos, M. de Melo Antunes, G. Guimarães, and S. M. M. de Lima e Silva, “Simultaneous Bayesian estimation of the temperature-dependent thermal properties of a metal slab using a three-dimensional transient experimental approach,” *International Journal of Thermal Sciences*, vol. 179, p. 107671, Sep. 2022, doi: 10.1016/j.ijthermalsci.2022.107671.

[59] D. S. Martínez, F. Illán, J. P. Solano, and A. Viedma, “Embedded thermocouple wall temperature measurement technique for scraped surface heat exchangers,” *Appl Therm Eng*, vol. 114, pp. 793–801, Mar. 2017, doi: 10.1016/j.applthermaleng.2016.12.039.

[60] G. D’Alessandro, F. de Monte, and D. E. Amos, “Effect of Heat Source and Imperfect Contact on Simultaneous Estimation of Thermal Properties of High-Conductivity Materials,” *Math Probl Eng*, vol. 2019, pp. 1–15, Jun. 2019, doi: 10.1155/2019/5945413.

[61] R. S. Graves, T. G. Kollie, D. L. McElroy, and K. E. Gilchrist, “The thermal conductivity of AISI 304L stainless steel,” *Int J Thermophys*, vol. 12, no. 2, pp. 409–415, Mar. 1991, doi: 10.1007/BF00500761.

[62] S. J. Chang, Y. Kang, B. Y. Yun, S. Yang, and S. Kim, “Assessment of effect of climate change on hygrothermal performance of cross-laminated timber building envelope with modular construction,” *Case Studies in Thermal Engineering*, vol. 28, p. 101703, Dec. 2021, doi: 10.1016/j.csite.2021.101703.

[63] M. Kamali and K. Hewage, “Development of performance criteria for sustainability evaluation of modular versus conventional construction methods,” *J Clean Prod*, vol. 142, pp. 3592–3606, Jan. 2017, doi: 10.1016/j.jclepro.2016.10.108.

[64] M. Kamali and K. Hewage, “Life cycle performance of modular buildings: A critical review,” *Renewable and Sustainable Energy Reviews*, vol. 62, pp. 1171–1183, Sep. 2016, doi: 10.1016/j.rser.2016.05.031.

[65] K. Orlowski, K. Shanaka, and P. Mendis, “Manufacturing, Modeling, Implementation and Evaluation of a Weatherproof Seal for Prefabricated Construction,” *Buildings*, vol. 8, no. 9, p. 120, Aug. 2018, doi: 10.3390/buildings8090120.

[66] S. Van Linden and N. Van Den Bossche, “Watertightness performance of face-sealed versus drained window-wall interfaces,” *Build Environ*, vol. 196, p. 107824, Jun. 2021, doi: 10.1016/j.buildenv.2021.107824.

[67] C. H. Lozinsky and M. F. Touchie, “Quantifying suite-level airtightness in newly constructed multi-unit residential buildings using guarded suite-level air leakage testing,” *Build Environ*, vol. 236, p. 110273, May 2023, doi: 10.1016/j.buildenv.2023.110273.

[68] C. H. Lozinsky and M. F. Touchie, “Improving energy model calibration of multi-unit residential buildings through component air infiltration testing,” *Build Environ*, vol. 134, pp. 218–229, Apr. 2018, doi: 10.1016/j.buildenv.2018.02.040.

[69] A. M. Tanyer, A. Tavukcuoglu, and M. Bekboliev, “Assessing the airtightness performance of container houses in relation to its effect on energy efficiency,” *Build Environ*, vol. 134, pp. 59–73, Apr. 2018, doi: 10.1016/j.buildenv.2018.02.026.

[70] S. Panico, M. Larcher, V. Marincioni, A. Troi, C. Baglivo, and P. M. Congedo, “Identifying key parameters through a sensitivity analysis for realistic hygrothermal simulations at wall level supported by monitored data,” *Build Environ*, vol. 229, p. 109969, Feb. 2023, doi: 10.1016/j.buildenv.2022.109969.

[71] M. Ruiz, V. Masson, M. Bonhomme, and S. Ginestet, “Numerical method for solving coupled heat and mass transfer through walls for future integration into an urban climate model,” *Build Environ*, vol. 231, p. 110028, Mar. 2023, doi: 10.1016/j.buildenv.2023.110028.

[72] S. Panico, M. Larcher, D. Herrera Avellanosa, C. Baglivo, A. Troi, and P. Maria Congedo, “Hygrothermal simulation challenges: Assessing boundary condition choices in retrofitting historic European buildings,” *Energy Build*, vol. 297, p. 113464, Oct. 2023, doi: 10.1016/j.enbuild.2023.113464.

[73] I. Vandemeulebroucke, S. Caluwaerts, and N. Van Den Bossche, “Decision framework to select moisture reference years for hygrothermal simulations,” *Build Environ*, vol. 218, p. 109080, Jun. 2022, doi: 10.1016/j.buildenv.2022.109080.

[74] W. Dong, Y. Chen, Y. Bao, and A. Fang, “A validation of dynamic hygrothermal model with coupled heat and moisture transfer in porous building materials and envelopes,” *Journal of Building Engineering*, vol. 32, p. 101484, Nov. 2020, doi: 10.1016/j.jobe.2020.101484.

[75] G. Tlaiji, F. Pennec, S. Ouldboukhitine, M. Ibrahim, and P. Biwole, “Hygrothermal performance of multilayer straw walls in different climates,” *Constr Build Mater*, vol. 326, p. 126873, Apr. 2022, doi: 10.1016/j.conbuildmat.2022.126873.

[76] Q. Zhan, Y. Xiao, F. Musso, and L. Zhang, “Assessing the hygrothermal performance of typical lightweight steel-framed wall assemblies in hot-humid climate regions by monitoring and numerical analysis,” *Build Environ*, vol. 188, p. 107512, Jan. 2021, doi: 10.1016/j.buildenv.2020.107512.

[77] S. Rouchier, M. Rabouille, and P. Oberlé, “Calibration of simplified building energy models for parameter estimation and forecasting: Stochastic versus deterministic modelling,” *Build Environ*, vol. 134, pp. 181–190, Apr. 2018, doi: 10.1016/j.buildenv.2018.02.043.

[78] M. Labat, M. Woloszyn, G. Garnier, and J. J. Roux, “Dynamic coupling between vapour and heat transfer in wall assemblies: Analysis of measurements achieved under real climate,” *Build Environ*, vol. 87, pp. 129–141, May 2015, doi: 10.1016/j.buildenv.2015.01.022.

[79] H. Palani and A. Karatas, “Investigating the disparities between experimental and computational analyses of thermal performance in prefabricated wall panels,” *Appl Therm Eng*, vol. 236, p. 121568, Jan. 2024, doi: 10.1016/j.applthermaleng.2023.121568.

[80] S. Yu, X. Liu, Y. Li, S. He, Y. Yao, and S. Sun, “Experimental and numerical simulation study on hygrothermal migration of damaged envelope walls during wind-driven rain,” *Build Environ*, vol. 243, p. 110653, Sep. 2023, doi: 10.1016/j.buildenv.2023.110653.

[81] M. J. Sorgato, A. P. Melo, and R. Lamberts, “The effect of window opening ventilation control on residential building energy consumption,” *Energy Build*, vol. 133, pp. 1–13, Dec. 2016, doi: 10.1016/j.enbuild.2016.09.059.

[82] C. Feng and H. Janssen, “Hygric properties of porous building materials (VII): Full-range benchmark characterizations of three materials,” *Build Environ*, vol. 195, p. 107727, May 2021, doi: 10.1016/j.buildenv.2021.107727.

[83] U. Berardi and M. Naldi, “The impact of the temperature dependent thermal conductivity of insulating materials on the effective building envelope performance,” *Energy Build*, vol. 144, pp. 262–275, Jun. 2017, doi: 10.1016/j.enbuild.2017.03.052.

[84] G. Giada, R. Caponetto, and F. Nocera, “Hygrothermal Properties of Raw Earth Materials: A Literature Review,” *Sustainability*, vol. 11, no. 19, p. 5342, Sep. 2019, doi: 10.3390/su11195342.

[85] Y. Wang, C. Ma, Y. Liu, D. Wang, and J. Liu, “Effect of moisture migration and phase change on effective thermal conductivity of porous building materials,” *Int J Heat Mass Transf*, vol. 125, pp. 330–342, Oct. 2018, doi: 10.1016/j.ijheatmasstransfer.2018.04.062.

[86] J. Piggot-Navarrete, P. Blanchet, M. R. Cabral, and C. Perez, “Investigating the impact of construction workmanship defects on the hygrothermal performance and airtightness of lightweight-structure wooden envelope systems,” *Build Environ*, vol. 243, p. 110705, Sep. 2023, doi: 10.1016/j.buildenv.2023.110705.

[87] A. A. Alvarado-Alvarado, A. De Bock, T. Ysebaert, B. Belmans, and S. Denys, “Modeling the hygrothermal behavior of green walls in Comsol Multiphysics®: Validation against measurements in a climate chamber,” *Build Environ*, vol. 238, p. 110377, Jun. 2023, doi: 10.1016/j.buildenv.2023.110377.

[88] R. Belloum, B. Agoudjil, N. Chennouf, and A. Boudenne, “Hygrothermal performance assessment of a bio-based building made with date palm concrete walls,” *Build Environ*, vol. 223, p. 109467, Sep. 2022, doi: 10.1016/j.buildenv.2022.109467.

[89] T. Colinart, D. Lelievre, and P. Glouannec, “Experimental and numerical analysis of the transient hygrothermal behavior of multilayered hemp concrete wall,” *Energy Build*, vol. 112, pp. 1–11, Jan. 2016, doi: 10.1016/j.enbuild.2015.11.027.

[90] D. Wu, M. Rahim, M. El Ganaoui, R. Djedjig, R. Bennacer, and B. Liu, “Experimental investigation on the hygrothermal behavior of a new multilayer building envelope integrating PCM with bio-based material,” *Build Environ*, vol. 201, p. 107995, Aug. 2021, doi: 10.1016/j.buildenv.2021.107995.

[91] M. Sawadogo, F. Benmahiddine, A. Godin, M. Duquesne, R. Belarbi, and A. Hamami, “Development and hygrothermal performance analysis of a novel eco-friendly insulating wall under various climatic conditions,” *Build Environ*, vol. 245, p. 110841, Nov. 2023, doi: 10.1016/j.buildenv.2023.110841.

[92] Q. Zhan, V. Pungercar, F. Musso, H. Ni, and Y. Xiao, “Hygrothermal investigation of lightweight steel-framed wall assemblies in hot-humid climates: Measurement and simulation validation,” *Journal of Building Engineering*, vol. 42, p. 103044, Oct. 2021, doi: 10.1016/j.jobe.2021.103044.

[93] A. Sadłowska-Sałęga and J. Radoń, “Feasibility and limitation of calculative determination of hygrothermal conditions in historical buildings: Case study of st. Martin church in Wiśniowa,” *Build Environ*, vol. 186, p. 107361, Dec. 2020, doi: 10.1016/j.buildenv.2020.107361.

[94] M. G. Gomes, A. M. Rodrigues, J. A. Bogas, and A. Freitas, “Thermophysical properties under different hygroscopic conditions of an innovative composite concrete pre-walls system,” *Constr Build Mater*, vol. 307, p. 124938, Nov. 2021, doi: 10.1016/j.conbuildmat.2021.124938.

[95] M. Ibrahim, H. Sayegh, L. Bianco, and E. Wurtz, “Hygrothermal performance of novel internal and external super-insulating systems: In-situ experimental study and 1D/2D numerical modeling,” *Appl Therm Eng*, vol. 150, pp. 1306–1327, Mar. 2019, doi: 10.1016/j.applthermaleng.2019.01.054.

[96] I. Costa-Carrapiço, B. Croxford, R. Raslan, and J. Neila González, “Hygrothermal calibration and validation of vernacular dwellings: A genetic algorithm-based optimisation methodology,” *Journal of Building Engineering*, vol. 55, p. 104717, Sep. 2022, doi: 10.1016/j.jobe.2022.104717.

[97] J. Ren, Z. Zhao, J. Zhang, J. Wang, S. Guo, and J. Sun, “Study on the hygrothermal properties of a Chinese solar greenhouse with a straw block north wall,” *Energy Build*, vol. 193, pp. 127–138, Jun. 2019, doi: 10.1016/j.enbuild.2019.03.040.

[98] K. A. Sabapathy and S. Gedupudi, “In situ thermal characterization of rice straw envelope of an outdoor test room,” *Journal of Building Engineering*, vol. 33, p. 101416, Jan. 2021, doi: 10.1016/j.jobe.2020.101416.

[99] S. Rouchier, M. Woloszyn, Y. Kedowide, and T. Béjat, “Identification of the hygrothermal properties of a building envelope material by the covariance matrix adaptation evolution strategy,” *J Build Perform Simul*, vol. 9, no. 1, pp. 101–114, Jan. 2016, doi: 10.1080/19401493.2014.996608.

[100] A. Jumabekova, J. Berger, A. Foucquier, and G. S. Dulikravich, “Searching an optimal experiment observation sequence to estimate the thermal properties of a multilayer wall under real climate conditions,” *Int J Heat Mass Transf*, vol. 155, p. 119810, Jul. 2020, doi: 10.1016/j.ijheatmasstransfer.2020.119810.

[101] A. Al-Omari, X. Brunetaud, K. Beck, and M. Al-Mukhtar, “Coupled thermal–hygric characterisation of elastic behaviour for soft and porous limestone,” *Constr Build Mater*, vol. 62, pp. 28–37, Jul. 2014, doi: 10.1016/j.conbuildmat.2014.03.029.

[102] J. Berger, D. Dutykh, and N. Mendes, “On the optimal experiment design for heat and moisture parameter estimation,” *Exp Therm Fluid Sci*, vol. 81, pp. 109–122, Feb. 2017, doi: 10.1016/j.expthermflusci.2016.10.008.

[103] N. P. Ramos, M. de M. Antunes, and S. M. M. de Lima e Silva, “Complementary transient thermal models and metaheuristics to simultaneously identify linearly temperature-dependent thermal properties of austenitic stainless steels,” *Phys Scr*, vol. 97, no. 11, p. 115006, Nov. 2022, doi: 10.1088/1402-4896/ac99ac.

[104] E. Julien, P. Blanchet, and L. Gosselin, “Case-Study: Fully Prefabricated Wood Wall Connection to Improve Building Envelope and On-Site Efficiency,” *Buildings*, vol. 12, no. 12, p. 2185, Dec. 2022, doi: 10.3390/buildings12122185.

[105] P. Armand, J. C. Gilbert, and S. Jan-Jégou, “A Feasible BFGS Interior Point Algorithm for Solving Convex Minimization Problems,” *SIAM Journal on Optimization*, vol. 11, no. 1, pp. 199–222, Jan. 2000, doi: 10.1137/S1052623498344720.

[106] M. Woloszyn and C. Rode, “Tools for performance simulation of heat, air and moisture conditions of whole buildings,” *Build Simul*, vol. 1, no. 1, pp. 5–24, Mar. 2008, doi: 10.1007/s12273-008-8106-z.

[107] C. Balocco, G. Petrone, and G. Cammarata, “Numerical multi-physical approach for the assessment of coupled heat and moisture transfer combined with people movements in historical buildings,” *Build Simul*, vol. 7, no. 3, pp. 289–303, Jun. 2014, doi: 10.1007/s12273-013-0146-3.

[108] M. Autengruber, M. Lukacevic, and J. Füssl, “Finite-element-based moisture transport model for wood including free water above the fiber saturation point,” *Int J Heat Mass Transf*, vol. 161, p. 120228, Nov. 2020, doi: 10.1016/j.ijheatmasstransfer.2020.120228.

[109] N. P. Ramos, M. de M. Antunes, and S. M. M. de Lima e Silva, “Complementary transient thermal models and metaheuristics to simultaneously identify linearly temperature-dependent thermal properties of austenitic stainless steels,” *Phys Scr*, vol. 97, no. 11, p. 115006, Nov. 2022, doi: 10.1088/1402-4896/ac99ac.

[110] C. Xu, S. Li, and K. Zou, “Study of heat and moisture transfer in internal and external wall insulation configurations,” *Journal of Building Engineering*, vol. 24, p. 100724, Jul. 2019, doi: 10.1016/j.jobe.2019.02.016.

[111] H. J. Moon, S. H. Ryu, and J. T. Kim, “The effect of moisture transportation on energy efficiency and IAQ in residential buildings,” *Energy Build*, vol. 75, pp. 439–446, Jun. 2014, doi: 10.1016/j.enbuild.2014.02.039.

[112] L. P. Thomas, B. M. Marino, and N. Muñoz, “Steady-state and time-dependent heat fluxes through building envelope walls: A quantitative analysis to determine their relative significance all year round,” *Journal of Building Engineering*, vol. 29, p. 101122, May 2020, doi: 10.1016/j.jobe.2019.101122.

[113] Z. A. Al-Absi, M. I. M. Hafizal, and M. Ismail, “Experimental study on the thermal performance of PCM-based panels developed for exterior finishes of building walls,” *Journal of Building Engineering*, vol. 52, p. 104379, Jul. 2022, doi: 10.1016/j.jobe.2022.104379.

[114] R. F. Rupp, N. G. Vásquez, and R. Lamberts, “A review of human thermal comfort in the built environment,” *Energy Build*, vol. 105, pp. 178–205, Oct. 2015, doi: 10.1016/j.enbuild.2015.07.047.

[115] M. Nadarajan and V. Kirubakaran, “Simulation studies on small rural residential houses using sustainable building materials for thermal comfort – case comparison,” *Advances in Building Energy Research*, vol. 11, no. 2, pp. 193–207, Jul. 2017, doi: 10.1080/17512549.2016.1215260.

[116] R. Caro and J. J. Sendra, “Are the dwellings of historic Mediterranean cities cold in winter? A field assessment on their indoor environment and energy performance,” *Energy Build*, vol. 230, p. 110567, Jan. 2021, doi: 10.1016/j.enbuild.2020.110567.

[117] X. Jin, X. Zhang, Y. Cao, and G. Wang, “Thermal performance evaluation of the wall using heat flux time lag and decrement factor,” *Energy Build*, vol. 47, pp. 369–374, Apr. 2012, doi: 10.1016/j.enbuild.2011.12.010.

[118] I. Danielski and M. Fröling, “Diagnosis of Buildings’ Thermal Performance - A Quantitative Method Using Thermography Under Non-steady State Heat Flow,” *Energy Procedia*, vol. 83, pp. 320–329, Dec. 2015, doi: 10.1016/j.egypro.2015.12.186.

[119] J. Berger and B. Kadoch, “Estimation of the thermal properties of an historic building wall by combining modal identification method and optimal experiment design,” *Build Environ*, vol. 185, p. 107065, Nov. 2020, doi: 10.1016/j.buildenv.2020.107065.

[120] Y. Yang, Z. Chen, T. Vogt Wu, A. Sempey, and J.-C. Batsale, “In situ methodology for thermal performance evaluation of building wall: A review,” *International Journal of Thermal Sciences*, vol. 181, p. 107687, Nov. 2022, doi: 10.1016/j.ijthermalsci.2022.107687.

[121] S. Cai, B. Zhang, and L. Cremaschi, “Review of moisture behavior and thermal performance of polystyrene insulation in building applications,” *Build Environ*, vol. 123, pp. 50–65, Oct. 2017, doi: 10.1016/j.buildenv.2017.06.034.

[122] J. Alencastro, A. Fuertes, and P. de Wilde, “The relationship between quality defects and the thermal performance of buildings,” *Renewable and Sustainable Energy Reviews*, vol. 81, pp. 883–894, Jan. 2018, doi: 10.1016/j.rser.2017.08.029.

[123] T. Theodosiou, K. Tsikaloudaki, K. Kontoleon, and C. Giarma, “Assessing the accuracy of predictive thermal bridge heat flow methodologies,” *Renewable and Sustainable Energy Reviews*, vol. 136, p. 110437, Feb. 2021, doi: 10.1016/j.rser.2020.110437.

[124] B. Mobaraki, F. J. Castilla Pascual, F. Lozano-Galant, J. A. Lozano-Galant, and R. Porras Soriano, “In situ U-value measurement of building envelopes through continuous low-cost monitoring,” *Case Studies in Thermal Engineering*, vol. 43, p. 102778, Mar. 2023, doi: 10.1016/j.csite.2023.102778.

[125] L. Yang, Y. Qiao, Y. Liu, X. Zhang, C. Zhang, and J. Liu, “A kind of PCMs-based lightweight wallboards: Artificial controlled condition experiments and thermal design method investigation,” *Build Environ*, vol. 144, pp. 194–207, Oct. 2018, doi: 10.1016/j.buildenv.2018.08.020.

[126] P. T. Tsilingiris, “Wall heat loss from intermittently conditioned spaces—The dynamic influence of structural and operational parameters,” *Energy Build*, vol. 38, no. 8, pp. 1022–1031, Aug. 2006, doi: 10.1016/j.enbuild.2005.11.012.

[127] T. Pilet and T. Rakha, “Modeling of transient conduction in building envelope assemblies: A review,” *Sci Technol Built Environ*, vol. 28, no. 6, pp. 706–716, Jul. 2022, doi: 10.1080/23744731.2022.2068315.

[128] N. Bishara, G. Pernigotto, A. Prada, M. Baratieri, and A. Gasparella, “Experimental determination of the building envelope’s dynamic thermal characteristics in consideration of hygrothermal modelling – Assessment of methods and sources of uncertainty,” *Energy Build*, vol. 236, p. 110798, Apr. 2021, doi: 10.1016/j.enbuild.2021.110798.

[129] N. C. Balaji, M. Mani, and B. V. Venkatarama Reddy, “Dynamic thermal performance of conventional and alternative building wall envelopes,” *Journal of Building Engineering*, vol. 21, pp. 373–395, Jan. 2019, doi: 10.1016/j.jobe.2018.11.002.

[130] Z. Fang and Y. Chen, “Applicability of the transfer function method and periodic response factors method in coincident design weather data generation,” *Energy Build*, vol. 250, p. 111254, Nov. 2021, doi: 10.1016/j.enbuild.2021.111254.

[131] F. Tariku and F. Hemmati, “RC-Network based thermal bridge calculation method for transient heat transfer analysis of multidimensional building envelope details: A frequency response analysis-based method,” *Energy Build*, vol. 300, p. 113648, Dec. 2023, doi: 10.1016/j.enbuild.2023.113648.

[132] S. Zhou, F. Bai, G. Razaqpur, and B. Wang, “Effect of key parameters on the transient thermal performance of a building envelope with Trombe wall containing phase change material,” *Energy Build*, vol. 284, p. 112879, Apr. 2023, doi: 10.1016/j.enbuild.2023.112879.

[133] S. Zhang, L. Yang, B. Suonam, H. Dong, and Y. Liu, “Method for dynamic thermal insulation design revealing almost real heat transfer characteristics of building envelopes in different Chinese regions,” *Energy Build*, vol. 274, p. 112419, Nov. 2022, doi: 10.1016/j.enbuild.2022.112419.

[134] R. G. Martinez, A. Riverola, and D. Chemisana, “Disaggregation process for dynamic multidimensional heat flux in building simulation,” *Energy Build*, vol. 148, pp. 298–310, Aug. 2017, doi: 10.1016/j.enbuild.2017.05.029.

[135] D. Mazzeo, G. Oliveti, and N. Arcuri, “A Method for Thermal Dimensioning and for Energy Behavior Evaluation of a Building Envelope PCM Layer by Using the Characteristic Days,” *Energies (Basel)*, vol. 10, no. 5, p. 659, May 2017, doi: 10.3390/en10050659.

[136] P. K. S. Rathore, S. K. Shukla, and N. K. Gupta, “Yearly analysis of peak temperature, thermal amplitude, time lag and decrement factor of a building envelope in tropical climate,” *Journal of Building Engineering*, vol. 31, p. 101459, Sep. 2020, doi: 10.1016/j.jobe.2020.101459.

[137] G. Vox, I. Blanco, F. Convertino, and E. Schettini, “Heat transfer reduction in building envelope with green façade system: A year-round balance in Mediterranean climate conditions,” *Energy Build*, vol. 274, p. 112439, Nov. 2022, doi: 10.1016/j.enbuild.2022.112439.

[138] S. Rouchier, “Solving inverse problems in building physics: An overview of guidelines for a careful and optimal use of data,” *Energy Build*, vol. 166, pp. 178–195, May 2018, doi: 10.1016/j.enbuild.2018.02.009.

[139] Q. Zhou and F. Xue, “Pushing the boundaries of modular-integrated construction: A symmetric skeleton grammar-based multi-objective optimization of passive design for energy savings and daylight autonomy,” *Energy Build*, vol. 296, p. 113417, Oct. 2023, doi: 10.1016/j.enbuild.2023.113417.

[140] H. Palani and A. Karatas, “Investigating the disparities between experimental and computational analyses of thermal performance in prefabricated wall panels,” *Appl Therm Eng*, vol. 236, p. 121568, Jan. 2024, doi: 10.1016/j.applthermaleng.2023.121568.

[141] D. Hong, G. Li, L. Wei, and Z. Yi, “An improved sequential function specification coupled with Broyden combined method for determination of transient temperature field of the steel billet,” *Int J Heat Mass Transf*, vol. 186, p. 122489, May 2022, doi: 10.1016/j.ijheatmasstransfer.2021.122489.

[142] S. Sun, Z. Chang, Y. Ji, G. Wang, and L. Wei, “Inverse Estimation of Transient Heat Flux Using Sequential Function Specification Method,” *Heat Transfer Engineering*, pp. 1–11, Mar. 2023, doi: 10.1080/01457632.2023.2185488.

[143] Y. Wang, N. Wang, and Q. Ren, “Predicting surface heat flux on complex systems via Conv-LSTM,” *Case Studies in Thermal Engineering*, vol. 33, p. 101927, May 2022, doi: 10.1016/j.csite.2022.101927.

[144] F. Wang, P. Zhang, Y. Wang, C. Sun, and X. Xia, “Real-time identification of severe heat loads over external interface of lightweight thermal protection system,” *Thermal Science and Engineering Progress*, vol. 37, p. 101583, Jan. 2023, doi: 10.1016/j.tsep.2022.101583.

[145] K. A. Woodbury, H. Najafi, F. Monte, and J. V. Beck, *Inverse Heat Conduction*. Wiley, 2023. doi: 10.1002/9781119840220.

[146] K. A. Woodbury and S. K. Thakur, “Redundant data and future times in the inverse heat conduction problem,” *Inverse Problems in Engineering*, vol. 2, no. 4, pp. 319–333, Jul. 1996, doi: 10.1080/174159796088027610.

[147] K. A. Woodbury and J. V. Beck, “Estimation metrics and optimal regularization in a Tikhonov digital filter for the inverse heat conduction problem,” *Int J Heat Mass Transf*, vol. 62, pp. 31–39, Jul. 2013, doi: 10.1016/j.ijheatmasstransfer.2013.02.052.

[148] W. J. Minkowycz, E. M. Sparrow, and J. Y. Murthy, Eds., *Handbook of Numerical Heat Transfer*. Wiley, 2000. doi: 10.1002/9780470172599.

[149] B. Blackwell and J. V. Beck, “A technique for uncertainty analysis for inverse heat conduction problems,” *Int J Heat Mass Transf*, vol. 53, no. 4, pp. 753–759, Jan. 2010, doi: 10.1016/j.ijheatmasstransfer.2009.10.014.